working electrode, a platinum-wire counter electrode, and a saturated calomel reference electrode; the reference electrode was in contact through a cracked bead well filled with electrolyte solution. The sample was weighed into the cell, the cell was flushed with nitrogen, and a known volume of the electrolyte solution (CH_2Cl_2, 0.1 M tetrabutylammonium perchlorate) was introduced via syringe. The voltammogram was run with use of a PAR Model 175 programmer hooked up to a PAR Model 173 potentiostat and a PAR Model 197 coulometer and I/V converter. The working electrode was polished after each run. Cyclic voltammograms at low temperature were run by cooling the cell in a dry-ice–acetone bath and allowing temperature equilibration for at least 15 min.

Acknowledgment. Financial support from the National Science Foundation is gratefully acknowledged.

Tripodal Polyphosphine Ligands in Homogeneous Catalysis. 1. Hydrogenation and Hydroformylation of Alkynes and Alkenes Assisted by Organorhodium Complexes with $MeC(CH_2PPh_2)_3$

Claudio Bianchini,* Andrea Meli, Maurizio Peruzzini, and Francesco Vizza

Istituto per lo Studio della Stereochimica ed Energetica dei Composti di Coordinazione, ISSECC CNR, Via J. Nardi 39, 50132 Firenze, Italy

Piero Frediani

Dipartimento di Chimica Organica, Università degli Studi di Firenze, Firenze, Italy

José A. Ramirez

Department of Chemistry, University of Valencia, Valencia, Spain

Received April 3, 1989

The crystal structure of the complex $[(triphos)RhCl(C_2H_4)]$ (1) has been determined by X-ray methods (triphos = $MeC(CH_2PPh_2)_3$). The rhodium atom is coordinated to an ethylene molecule, a chlorine atom, and the triphos ligand, which occupies three *fac* positions of an octahedron. The Rh–C_2H_4 coordination exhibits a C–C distance that is among the longest found in metal–ethylene structures (1.49 (4) Å). Compound 1 is the starting point to synthesize a number of ethylene complexes of rhodium containing hydride or σ-organyl coligands: $[(triphos)RhH(C_2H_4)]$, $[(triphos)Rh(C_2H_5)(C_2H_4)]$, $[(triphos)Rh(CH_3)(C_2H_4)]$, $[(triphos)Rh(C_6H_5)(C_2H_4)]$. All of the ethylene complexes but 1 react with CO, forming σ-acyl carbonyls of general formula [(triphos)Rh(COR)(CO)] via the σ-organyl carbonyls [(triphos)Rh(R)(CO)] (R = CH_3, C_2H_5, C_6H_5). Compound 1 reacts with CO, yielding the carbonyl [(triphos)RhCl(CO)]. The hydrogenolysis reactions of the σ-organyl ethylene complexes invariably give the trihydride $[(triphos)Rh(H)_3]$ and the corresponding hydrocarbon. In contrast, the σ-acyl carbonyls and the σ-organyl carbonyls react with H_2 to form the hydride carbonyl [(triphos)RhH(CO)] and the corresponding hydrocarbon or aldehyde. Another excellent synthetic entry to organorhodium complexes of triphos is the η^2-alkyne complex $[(triphos)Rh(\eta^2\text{-DMAD})]BPh_4$ (DMAD = dimethyl acetylenedicarboxylate). This reacts with H_2 to give the tetrahydride $[(triphos)RhH(\mu\text{-}H)_2HRh(triphos)](BPh_4)_2$ and dimethyl succinate. Reaction of the η^2-alkyne complex with CO affords the dicarbonyl $[(triphos)Rh(CO)_2]BPh_4$ which is converted into the ethylene carbonyl $[(triphos)Rh(CO)(C_2H_4)]BPh_4$ by treatment with Me_3NO under a C_2H_4 atmosphere. The ethylene carbonyl is much better synthesized by protonation of [(triphos)RhH(CO)] under C_2H_4. In the absence of ethylene, the reaction gives $[(triphos)Rh(H)_2(CO)]BPh_4$. The hydrogenolysis and carbonylation reactions have been carried out at room temperature and 1 atm of H_2 or CO. All of the compounds have been properly characterized by spectroscopic technique, including the computer simulation of the second-order ^1H and ^{31}P NMR spectra. The activities of all of the compounds as catalyst precursors for the homogeneous hydrogenation, isomerization, and hydroformylation reactons of alkenes and alkynes have been studied in detail. Particular attention has been focused on the substrates 1-hexene, *cis*-stilbene, diphenylacetylene, dimethyl maleate, and dimethyl acetylenedicarboxylate.

Introduction

Over the past decade, tripodal polyphosphines have proven to be useful and versatile ligands in inorganic and organometallic chemistry.[1] Recently, transition-metal complexes of tripodal polyphosphines have begun to attract interest because of their potential as catalysts in several homogeneous reactions, including (i) hydrogenation of alkynes, alkenes,[2] and organic nitriles,[2d,3] (ii) hydroformylation and isomerization of alkenes,[2b-h] (iii) acetalization of aldehydes and ketones,[2d,4] (iv) functionalizaton, oligomerization, and polymerization of alkynes,[5] (v) oxidation of inorganic and organic substrates,[6] and (vi) synthesis of vinyl ethers from terminal alkynes and carboxylic acids.[7] The principal reasons tripodal polyphosphine ligands participate in such a wide range of catalyst systems can be summarized under six main headings:[8] excellent bonding ability, strong trans influence, formation of stable complexes in a variety of metal oxidation states, great control on the stereochemistry and stoichiometry, adaptability to many different coordination numbers, and high nucleophilicity of the metal centers.

The majority of studies have involved the triphosphine triphos, $MeC(CH_2PPh_2)_3$ (I), which can form stable com-

0276-7333/90/2309-0226$02.50/0

plexes with most d-block metals in a variety of stereochemistries.[1a-c] In all cases, however, triphos occupies

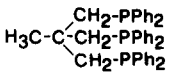

I

three facial sites on the coordination polyhedra. A metal that proves particularly suitable for being coordinated by triphos is rhodium in all of its formal oxidation states. In particular, the (triphos)Rh system can readily enter into the metal III → I → III oxidation/reduction cycle with no phosphine arm dissociation or apparent destabilization of the resulting complexes.[9] This is a very important point, as rhodium contributes the essential ingredient in several catalyst systems for which the metal III → I → III oxidation/reduction cycle is an essential requisite.

Depending on the oxidation state of rhodium, the (triphos)Rh fragment can be saturated by two or three coligands to give either mononuclear or binuclear complexes. With very few exceptions,[10] mononuclear complexes of Rh(III) are octahedral (II).[11] In contrast, those of Rh(I) may adopt either square-pyramidal (III) or trigonal-bipyramidal (IV) geometries.[11a,12] When the unsaturated rhodium fragments are stabilized by dimerizaton, binuclear species with two (V) or three (VI) bridging ligands can be obtained.[13,14]

Table I. Selected $^{31}P\{^1H\}$ NMR Data[a]

compd	pattern	chem shift, ppm $\delta(P_A)$	chem shift, ppm $\delta(P_M)$	coupling constant, Hz PP	coupling constant, Hz P_ARh	coupling constant, Hz P_MRh
1	AM_2X	45.73	-10.79	28.4	130.9	110.9
2	AM_2X	14.43	18.18	33.0	82.9	132.7
3	AB_2X	8.45	8.90	31.1	74.2	131.2
4	AB_2X	8.97	7.12	31.9	78.2	126.2
5	AM_2X	11.89	0.25	30.7	71.0	123.7
6	A_3X	5.34			110.1	
	AM_2X[b]	15.60	1.20	42.6	71.8	129.6
7[c]	A_3X	4.51			113.1	
	AM_2X[b]	13.40	0.60	42.7	72.0	131.5
8	A_3X	3.63			110.1	
	AM_2X[b]	17.18	-0.58	42.6	72.1	127.1
9[c]	A_3X	9.60			110.4	
	AM_2X[b]	24.20	2.36	42.0	80.1	123.2
10[c]	A_3X	11.50			114.8	
	AM_2X[b]	23.20	7.75	40.6	82.6	124.4
11[c]	A_3X	8.20			106.2	
	AM_2X[b]	24.20	2.06	40.6	76.4	124.2
12	AM_2X	48.92	-1.50	24.2	137.5	77.8
15[d]	A_3X	42.05			109.3	
18	A_3X	9.20			101.1	
	AM_2X[b]	24.38	2.50	43.9	86.4	108.0
19	AM_2X[d]	29.97	9.78	34.9	98.0	77.0

[a] CH_2Cl_2/CD_2Cl_2, 293 K. [b] 183 K. [c] THF/THF-d_8, 293 K. [d] CH_3COCH_3/CD_3COCD_3, 293 K.

II III IV

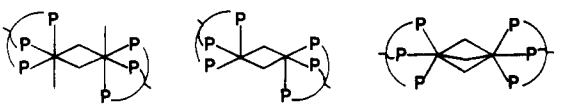

V VI

Whatever the structure may be, the (triphos)Rh moiety proves particularly suitable to coordinate *participative* ligands, i.e. ligands such as hydride, alkene, alkyl, and carbonyl, which take an active part in several important catalytic reactions.

In this paper we describe the synthesis and the chemical-physical properties of a number of new mononuclear organorhodium complexes of triphos. A detailed study on the hydrogenation reactions of various alkenes and alkynes and on the hydroformylation reactions of alkenes has been carried out. Also, we compare and contrast the catalytic activity of complexes containing *participative* ligands with that of (i) related mononuclear species containing *nonparticipative* ligands and (ii) related dirhodium complexes. This has provided precious mechanistic information on the catalytic processes.

A preliminary communication of part of this work has already appeared.[2c]

Results and Discussion

The preparations and the principal reactions of the complexes described in this paper are reported in Schemes

(1) (a) Sacconi, L.; Mani, F. *Transition Met. Chem. (N.Y.)* **1982**, *8*, 179. (b) Bianchini, C.; Mealli, C.; Meli, A.; Sabat, M. In *Stereochemistry of Organometallic and Inorganic Compounds*; Bernal, I., Ed.; Elsevier: Amsterdam, 1986; Vol. 1, p 146. (c) Bianchini, C. *Comments Inorg. Chem.* **1988**, *8*, 27. (d) Bianchini, C.; Masi, D.; Meli, A.; Peruzzini, M.; Zanobini, F. *J. Am. Chem. Soc.* **1988**, *110*, 6411. (e) Kerpot, D. G. E.; Mawby, R. J.; Sgamellotti, A.; Venanzi, L. M. *Inorg. Chim. Acta* **1974**, *8*, 195. (f) Siegl, W. O.; Lapporte, S. J.; Collmann, J. P. *Inorg. Chem.* **1973**, *12*, 674. (g) King, R. B.; Kapoor, R. M.; Soran, M. S.; Kapoor, P. N. *Inorg. Chem.* **1971**, *10*, 1851. (h) Geerts, R. L.; Huffmann, J. C.; Westerberg, D. E.; Folting, K.; Caulton, K. G. *New J. Chem.* **1988**, *12*, 455. (i) DuBois, D. L.; Miedaner, A. *Inorg. Chem.* **1986**, *25*, 4620. (j) Bianchini, C.; Mealli, C.; Peruzzini, M.; Zanobini, F. *J. Am. Chem. Soc.* **1987**, *109*, 5548. (k) Bianchini, C.; Laschi, F.; Meli, A.; Vacca, A.; Zanello, P. *J. Am. Chem. Soc.* **1988**, *27*, 3716. (l) Janser, P.; Venanzi, L. M.; Banchechi, F. J. *Organomet. Chem.* **1985**, *296*, 229. (m) Hommeltoft, S. I.; Baird, M. C. *J. Am.* Chem. *Soc.* **1985**, *107*, 2548. (n) Hommeltoft, S. I.; Baird, M. C. *Organometallics* **1986**, *5*, 190. (o) Rhodes, L. F.; Sorato, C.; Venanzi, L. M.; Bachechi, F. *Inorg. Chem.* **1988**, *27*, 604. (p) Dahlenburg, L.; Frosin, K.-M. *Chem. Ber.* **1988**, *121*, 865. (q) Antberg, M.; Dahlenburg, L.; Frosin, K-M.; Hock, N. *Chem. Ber.* **1988**, *121*, 859. (r) Antberg, M.; Frosin, K.-M.; Dahlenburg, L. *J. Organomet. Chem.* **1988**, *338*, 319. (s) Hohman, W. H.; Kountz, D. J.; Meek, D. W. *Inorg. Chem.* **1986**, *25*, 616.

(2) (a) DuBois, D. L.; Meek, D. W. *Inorg. Chim. Acta* **1976**, *19*, L29. (b) Bianchini, C.; Mealli, C.; Meli, A.; Peruzzini, M.; Zanobini, F. *J. Am. Chem. Soc.* **1988**, *110*, 8725. (c) Bianchini, C.; Meli, A.; Peruzzini, M.; Vizza, F.; Fujiwara, Y.; Jintoku, T.; Taniguchi, H. *J. Chem. Soc., Chem. Commun.* **1988**, 210. (d) Ott, J. Dissertation, ETH No. 8000, Zurich, Switzerland, 1986. (e) Bianchini, C.; Meli, A.; Laschi, F.; Ramirez, J. A.; Zanello, P. *Inorg. Chem.* **1988**, *27*, 4429. (f) Sanger, A. *J. Mol. Catal.* **1977/78**, *3*, 221. (g) Sanger, A. R.; Schallig, L. R. *J. Mol. Catal.* **1977/78**, *3*, 101. (h) Bianchini, C.; Laschi, F.; Meli, A.; Peruzzini, M.; Zanello, P.; Frediani, P. *Organometallics* **1988**, *7*, 2575.

(3) (a) Rhodes, L. F.; Venanzi, L. M. *Inorg. Chem.* **1987**, *26*, 2692. (b) Bianchini, C.; Meli, A.; Frediani, P. Manuscript in preparation.

(4) Ott, J.; Venanzi, L. M.; Wang, G. *Abstracts of Papers*, Fall Meeting of the Schweizerisch Chemische Gesellschaft, Bern, Switzerland, Oct 16, 1987; p 96.

(5) Bianchini, C.; Frediani, P.; Meli, A.; Vizza, F.; Peruzzini, M.; Zanobini, F. *Organometallics* **1989**, *8*, 2080.

(6) Bianchini, C.; Mealli, C.; Meli, A.; Peruzzini, M.; Proserpio, D. M.; Vizza, F.; Frediani, P. *J. Organomet. Chem.* **1989**, *369*, C6.

(7) Bianchini, C.; Meli, A.; Peruzzini, M.; Zanobini, F.; Bruneau, C.; Dixneuf, P. H. Submitted for publication.

(8) Meek, D. W. In *Homogeneous Catalysis with Metal Phosphine Complexes*; Pignolet, L. H., Ed.; Plenum Press: New York, 1983; p 257.

(9) Bianchini, C.; Meli, A.; Laschi, F.; Vizza, F.; Zanello, P. *Inorg. chem.* **1989**, *28*, 227.

(10) (a) Bianchini, C.; Masi, D.; Mealli, C.; Meli, A.; Sabat, M.; Vizza, F. *Inorg. Chem.* **1988**, *27*, 3716. (b) Bianchini, C.; Meli. A.; Dapporto, P.; Tofanari, A.; Zanello, P. *Inorg. Chem.* **1987**, *26*, 3677.

(11) (a) Ott, J.; Venanzi, L. M.; Ghilardi, C. A.; Midollini, S.; Orlandini, A. *J. Organomet. Chem.* **1985**, *291*, 89. (b) Bianchini, C.; Mealli, C.; Meli, A.; Sabat, M.; Silvestre, J.; Hoffmann, R. *Organometallics* **1986**, *5*, 1733.

(12) Dahlenburg, L. Mirzaei, F. *Inorg. Chim. Acta* **1985**, *97*, L1.

(13) Allevi, C.; Golding, M.; Heaton, B. T.; Ghilardi, C. A.; Midollini, S.; Orlandini, A. *J. Organomet. Chem.* **1987**, *236*, C19.

(14) (a) Cecconi, F.; Ghilardi, C. A.; Midollini, S.; Orlandini, A.; Zanello, P.; Heaton, B. T.; Huang, L.; Iggo, J. A.; Bordoni, S. *J. Organomet. Chem.* **1988**, *353*, C5. (b) Bianchini, C.; Mealli, C.; Meli, A.; Sabat, M. *Inorg. Chem.* **1986**, *25*, 4617. (c) Bianchini, C.; Mealli, C.; Meli, A.; Sabat, M. *J. Chem. Soc., Chem. Commun.* **1986**, 777.

Table II. Selected ^1H NMR Data[a]

	$H_2C=CH_2$						Rh—R					
	pattern	δ(A)	δ(B)	δ(C)	δ(D)	J, Hz	R	pattern	δ(A)	δ(B)	δ(C)	J, Hz
1	AA'BB'	3.15	1.71			9.8 (J(AB) + J(AB'))						
2[b]	AA'BB'	3.05	1.65			9.2 (J(AB)) 5.0 (J(AB'))	H	AMN_2X	−11.70			171.1 (J(AM)) 6.6 (J(AN)) 14.2 (J(AX))
3	AA'BB'	3.29	2.76			10.5 (J(AB) + J(AB'))	C_2H_5	A_3B_2X	1.18	0.40		6.6 (J(AB)) 5.1 (J(BX))
4	AA'BB'	2.64	2.16			11.0 (J(AB) + J(AB'))	CH_3	A_3MN_2X	−0.71			1.8 (J(AM)) 8.9 (J(AN)) 5.2 (J(aX))
5	ABCD	2.23	2.23	2.01	2.04	8.4 (J(AC) = J(AD))	C_6H_5	AA'BB'CX	7.56	6.41	6.50	7.1 (J(AB)) 6.8 (J(AB)) 6.8 (J(BC)) 1.7 (J(BX))
6							$COCH_3$	A_3	2.13			
7[c]							COC_2H_5	A_3B_2	1.13	2.53		7.2 (J(AB))
8							COC_6H_5	AA'BB'C	7.51	6.38	6.80	7.1 (J(AB)) 6.8 (J(BC)) 0.8 (J(AC))
9[c]							C_2H_5	$A_3B_2M_3X$	0.62	1.15		6.5 (J(AB)) 5.2 (J(BX)) 1.2 (J(AX)) 1.7 (J(BM))
10[c]							CH_3	A_3M_3X	−0.15			1.9 (J(AM)) 6.7 (J(AX))
11[c]							C_6H_5	AA'BB'CX	7.52	6.53	6.63	7.1 (J(AB)) 6.8 (J(BC)) 0.9 (J(AC)) 6.8 (J(AX)) 2.7 (J(BX))
12							H	AA'XX'YZ	−7.35			*f*
18[d,e]		3.59	1.98			10.3 (J(AB) + J(AB'))						
19							H	AA'XX'YZ	−7.24			*f*

[a] CD_2Cl_2, 293 K. [b] −10 °C. [c] THF-d_8, 293 K. [d] CD_3COCD_3, 293 K. [e] −20 °C. [f] See text.

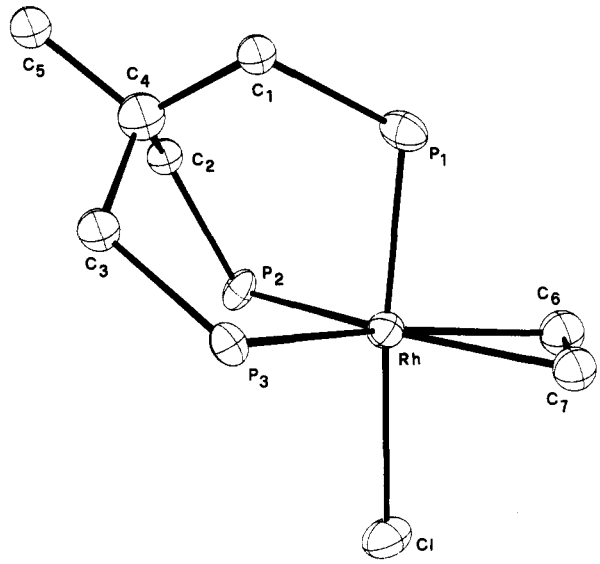

Figure 1. ORTEP drawing of complex 1. Hydrogen atoms of the alkyl chains and phenyl rings of triphos are omitted for clarity.

Table III. Selected Bond Distances (Å) and Angles (deg) for 1

Rh-Cl	2.462 (7)	P2-C2	1.83 (2)
Rh-P1	2.222 (7)	P3-C3	1.87 (2)
Rh-P2	2.352 (6)	C1-C4	1.54 (3)
Rh-P3	2.371 (6)	C2-C4	1.52 (3)
Rh-C6	2.20 (2)	C3-C4	1.54 (3)
Rh-C7	2.19 (2)	C4-C5	1.51 (4)
P1-C1	1.86 (2)	C6-C7	1.49 (4)
Cl-Rh-C6	83.5 (6)	P1-Rh-P3	88.9 (2)
Cl-Rh-C7	83.6 (6)	P2-Rh-P3	88.7 (2)
Rh-C6-C7	70 (1)	Rh-P1-C1	112.3 (7)
Rh-C7-C6	70 (1)	Rh-P2-C2	108.4 (7)
Cl-Rh-P1	173.2 (2)	Rh-P3-C3	107.8 (7)
Cl-Rh-P2	92.1 (2)	P1-C1-C4	114 (2)
Cl-Rh-P3	97.7 (2)	P2-C2-C4	119 (2)
C6-Rh-C7	39 (1)	P3-C3-C4	118 (2)
P1-Rh-C6	89.9 (6)	C1-C4-C2	113 (2)
P1-Rh-C7	92.5 (6)	C1-C4-C3	108 (2)
P2-Rh-C6	118.0 (7)	C2-C4-C3	111 (2)
P2-Rh-C7	157.5 (6)	C1-C4-C5	110 (2)
P3-Rh-C6	153.3 (8)	C2-C4-C5	109 (2)
P3-Rh-C7	113.8 (6)	C3-C4-C5	105 (2)
P1-Rh-P2	89.4 (2)		

I, II, IV, and V. Selected NMR data are collected in Tables I ($^{31}P\{^1H\}$ spectra) and II (^1H spectra). The most significant IR absorptions are given in the Experimental Section.

Synthesis and Characterization of Ethylene Complexes. [(triphos)RhCl(C_2H_4)]. The reaction of [Rh$Cl(C_2H_4)_2]_2$ with triphos in CH_2Cl_2 under 1 atm of C_2H_4 provides a clean, high-yield method for the synthesis of [(triphos)RhCl(C_2H_4)] (1), a key starting material for entering into the organometallic chemistry of rhodium with triphos. Compound 1 is fairly air-stable in the solid state but decomposes in solution unless air is excluded. It remains unchanged for days in solutions saturated with ethylene. The crystal structure of 1 has been determined by X-ray methods. An ORTEP drawing of the molecule is shown in Figure 1. Selected bond distances and angles are reported in Table III. The rhodium atom is coordinated to an ethylene molecule, a chlorine atom, and the triphos ligand, which occupies three *fac* positions of an octahedron (the three P–Rh–P angles are only a bit less than 90°). The Rh–P bond trans to the chloride atom is significantly shorter than the two Rh–P basal distances, 2.222 (7) vs 2.352 (6) and 2.371 (6) Å. The η^2-ethylene ligand is practically coplanar with the P3–Rh–P2 moiety, the dihedral angle between the two planes being 4 (1)°. The Rh–C_2H_4 coordination exhibits a C–C distance (1.49

(4) Å) that is among the longest found in metal–C_2H_4 structures, while the Rh–C distances (2.20 (2) and 2.19 (2) Å) are unusually short.[15] These and other geometrical parameters associated with ethylene ligation in **1** are consistent with a bonding involving considerable metal to ligand π-donation and, therefore, suggest a rhodacyclopropane structure.[16]

The solid-state structure of **1** seems to be maintained in solution as shown by the $^{31}P\{^1H\}$ NMR spectrum in CH_2Cl_2. This consists of an AM_2X spin system exhibiting spectroscopic parameters that are typical of octahedral rhodium complexes of triphos containing two equal ligands.[10] The spectrum is temperature invariant from −70 to +10° C, above which temperature the two resonances begin to broaden but remain practically unshifted (at +35 °C, the P_A resonance is completely unresolved; recording spectra at higher temperature is precluded because of considerable decomposition of the compound). In reality, a fluxional process of minor entity, most likely restricted to the (triphos)Rh moiety, appears to take place above 10 °C as the ^1H NMR spectrum in CD_2Cl_2 at room temperature shows a unique resonance, centered at 2.33 ppm, for the six CH_2 protons of triphos. Below 10 °C, the alkyl chains of the ligand become rigid and give rise to a typical series of sharp resonances between 2.4 and 2.1 ppm. The same effect is observed for the six phenyl substituents on the phosphorus donors. The ^1H NMR spectrum exhibits two "doublets" of equal intensity (2 H) at 3.15 and 1.71 ppm. This part of the spectrum is an AA′BB′ pattern with $N = J(AB) + J(AB)' = 9.8$ Hz and is assigned to the ethylene hydrogens, each pair of which resides in a different environment (VII).[17] The other parameters K, L, and M as well as eventual couplings to the phosphorus and rhodium nuclei could not be calculated because of the poor resolution of the spectrum. When the temperature is lowered, the spin system does not change, the only variation being an upfield shift of the AA′ portion from 1.71 to 1.44 ppm. Finally, in good agreement with the observed structure, a single ethylene carbon resonance at 30.5 ppm (J(CRh) = 13.5 Hz) is found in the $^{13}C\{^1H\}$ NMR spectrum of **1** (CD_2Cl_2, 20 °C).[18]

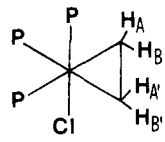

VII

[(triphos)RhH(C_2H_4)]. By treatment of **1** in THF with a slight excess of $LiHBEt_3$, followed by addition of 1-butanol, yellow crystals of [(triphos)RhH(C_2H_4)] (**2**) are obtained in excellent yield. Alternatively, **2** can be synthesized either by treating **1** with EtMgBr in THF, a reaction that proceeds via β-H elimination in the σ-ethyl complex [(triphos)Rh(C_2H_5)(C_2H_4)] (see below), or by refluxing the trihydride [(triphos)RhH_3] in THF under ethylene. Compound **2** is fairly stable in the solid state and in deaerated solutions, in which, like its chloride congener **1**, it is a nonconductor. The IR spectrum contains a medium-intensity band at 1965 cm^{-1} assigned to ν(Rh–H), thus evidencing that the Cl/H metathesis reaction has occurred. As far as the primary geometry is concerned, the hydride ethylene complex can be considered almost identical with the chloride ethylene parent compound. In fact, the $^{31}P\{^1H\}$ NMR spectrum of **2** consists of an AM_2X spin system, temperature invariant from −70 to +35 °C (the complex does not show any fluxionality). In accord with the stronger trans effect of hydride vs that of chloride, the $J(P_ARh)$ coupling constant is much smaller in **2** than in **1** (82.9 vs 130.9 Hz). The ethylene protons still give rise to an AA′BB′ pattern with J(AB) = 9.1 Hz and J(AB′) = 5.0 Hz. The hydride resonance falls in the usual range for Rh–hydride complexes (−11.70 ppm) and consists of a doublet of pseudoquintuplets, as expected for an HAM_2X system (Figure 2).

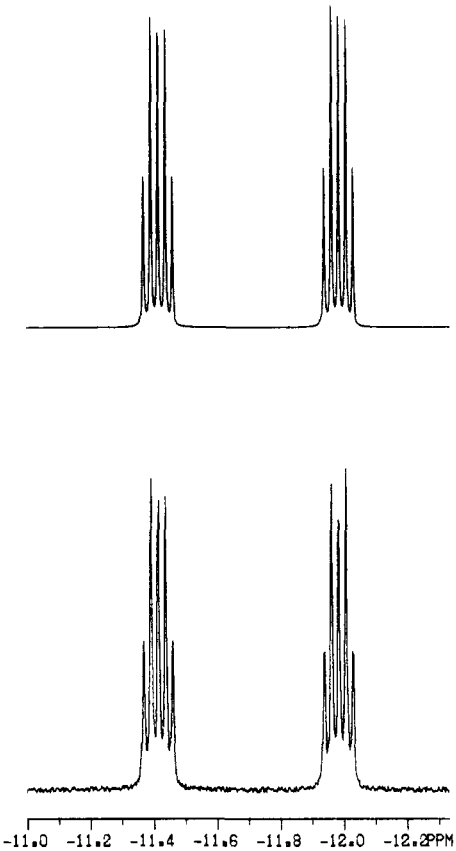

Figure 2. Experimental (bottom) and computed (top) ^1H NMR spectra in the hydride region of **2** (300 MHz, 293 K, CD_2Cl_2, TMS reference).

[(triphos)Rh(C_2H_5)(C_2H_4)]. When **1** in THF is reacted with either $LiHBEt_3$ or EtMgBr under 1 atm of C_2H_4, the subsequent addition of 1-butanol/n-heptane causes precipitation of pale yellow crystals of the σ-ethyl η^2-ethylene complex [(triphos)Rh(C_2H_5)(C_2H_4)] (**3**). Compound **3** is quantitatively prepared also by bubbling ethylene into a THF solution of **2**, thus clearly demonstrating that C_2H_4 addition promotes migration of hydrogen from the metal to the coordinated alkene.[19,20] Unlike the chloride or hydride congeners, **3** is stable in solution only under a C_2H_4 atmosphere. As a matter of fact, purging a solution of **3** with N_2 results in the fast formation of the hydride **2** and C_2H_4 evolution. No insertion of ethylene into the Rh–C(ethylene) bond is observed even at a very high pressure of C_2H_4 (40 atm). The proton NMR spectrum exhibits two multiplets at 0.40 ppm (2 H) and at 1.18 ppm (3 H) attributable to a σ-bonded ethyl group. This portion of the

(15) Carr, S. W.; Shaw, B. L.; Thornton-Pett, M. *J. Chem. Soc., Dalton Trans.* **1987**, 1763.
(16) Guggenberger, L. J.; Cramer, R. *J. Am. Chem. Soc.* **1972**, *94*, 3779.
(17) Emsley, J. M.; Feeney, J.; Sutcliffe, L. H. In *High Resolution Nuclear Magnetic Resonance Spectroscopy*; Pergamon Press: Oxford, U.K. 1965; Vol. 1.
(18) Guggenberger, L. J.; Meakin, P.; Tebbe, F. N. *J. Am. Chem. Soc.* **1974**, *96*, 5420.
(19) Doherty, N. M.; Bercaw, J. E. *J. Am. Chem. Soc.* **1985**, *107*, 2670.
(20) Werner, H.; Feser, R. *Angew. Chem., Int. Ed. Engl.* **1979**, *18*, 157.

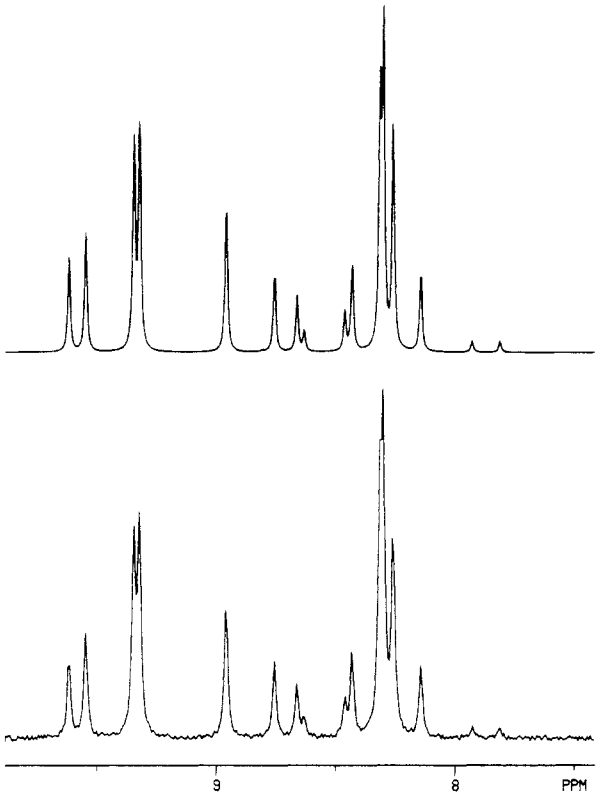

Figure 3. Experimental (bottom) and computed (top) $^{31}P\{^1H\}$ NMR spectra of 3 (121.42 MHz, 293 K, CD_2Cl_2, 85% H_3PO_4 reference).

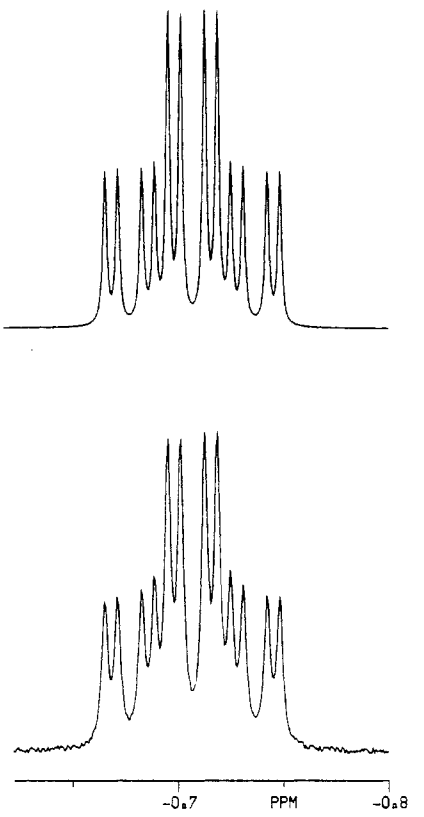

Figure 4. Experimental (bottom) and computed (top) ^1H NMR resonances due to the σ-methyl group in 4 (300 MHz, 293 K, CD_2Cl_2, TMS reference).

spectrum was tentatively simulated as the A_3B_2 part of an $A_3B_2MN_2X$ spin system. However, the poor resolution of the spectrum gave as the only reliable values $J(AB)$ and $J(BX)$ (see Table II). For the same reason, only $J(AB) + J(AB') = 10.5$ Hz can be provided for the ethylene hydrogens, which give rise to two "doublets" of equal intensity (2 H) at 3.29 and 2.76 ppm, respectively. Because of the presence of very similar groups, i.e. CH_2, trans to all of the three phosphorus atoms of triphos, the $^{31}P\{^1H\}$ NMR spectrum, shown in Figure 3, is now of the second-order AB_2X type with $\delta(P_A)$ very close to $\delta(P_B)$ (8.45 and 8.90 ppm, respectively). Interestingly, this provides further support for the metallacyclopropane type structure assigned to the present family of ethylene complexes (vide infra).

[(triphos)RhR(C_2H_4)] (R = CH_3, C_6H_5). Compound 1 in THF undergoes metathetical reactions with main-group organometallic compounds.[21] Thus, the methyl and phenyl derivatives [(triphos)Rh(CH_3)(C_2H_4)] (4) and [(triphos)Rh(C_6H_5)(C_2H_4)] (5) are obtained as yellow crystals. Both compounds are air-stable in the solid state and in deoxygenated solutions. The IR spectra do not provide much information, the only significant absorbance being exhibited by 5 at 1568 cm^{-1}, which is due to an additional ν(C–C) phenyl vibration.[1d] On the other hand, the presence of σ-bonded carbon ligands in both compounds is readily inferred by ^1H NMR spectroscopy. In particular, the spectrum of 4 contains a well-resolved multiplet at −0.71 ppm (3 H), which is absent in the spectrum of the starting chloride and has been assigned to a methyl ligand. As is shown in Figure 4, the three equivalent hydrogens of CH_3 can be simulated as the A part of an A_3MN_2X spin system, being coupled to the two basal phosphorus atoms, the apical phosphorus atom, and the rhodium nucleus.

In a similar way, the ^1H NMR spectrum of 5 exhibits a set of new bands in the aromatic proton region that are not present in the spectrum of 1. Such additional resonances form an AA'BB'CX system and are diagnostic for a σ-bonded phenyl group (VIII).

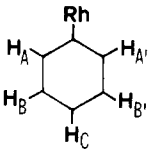

VIII

Interestingly, while the $^{31}P\{^1H\}$ NMR spectrum of 5 is of the first-order AM_2X type like those of 1 and 2, the spectrum of 4 (Figure 5) is a second-order AB_2X type like that of the ethyl congener 3. However, the second-order character is clearly less pronounced in 4 than in 3, most likely because the ligand trans to the apical phosphorus, i.e. CH_3, is less similar to the CH_2 ends of ethylene than the ethyl CH_2 group of 3. In accord with this interpretation, when the carbon ligand trans to the apical phosphorus is even more different, as the phenyl group in 5, a typically first-order AM_2X spectrum is observed.

As occurs for the very similar ethyl complex 3, the resonances of the C_2H_4 protons in 4 appear as two "doublets" at 2.64 and 2.16 ppm with $J(AB) + J(AB') = 11.0$ Hz. In contrast, the ethylene hydrogens in the phenyl derivative 5 originate as a doublet at 2.23 ppm (2 H) and two partially overlapping doublets at 2.01 and 2.04 ppm (1 H each). This pattern has been properly simulated as an ABCD spin system in which the A and B nuclei are isochronous. The nonequivalence of the four protons of C_2H_4 may be due to a slow rotation of the phenyl ring trans

(21) Klein, H.-F.; Hammer, R.; Gross, J.; Schubert, U. *Angew. Chem., Int. Ed. Engl.* **1980**, *19*, 809.

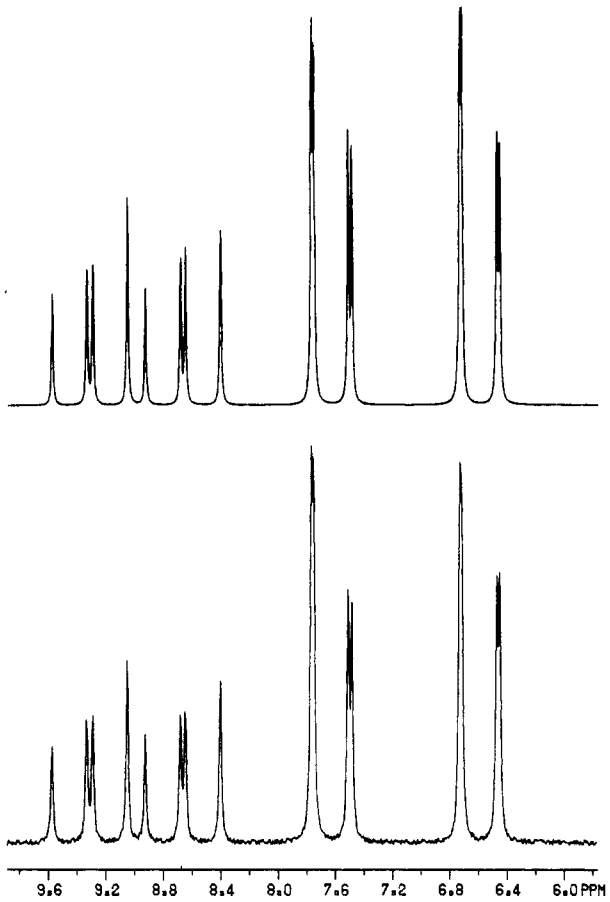

Figure 5. Experimental (bottom) and computed (top) $^{31}P\{^1H\}$ NMR spectra of **4** (121.42 MHz, 293 K, CD_2Cl_2, 85% H_3PO_4 reference).

to the apical phosphorus, a fact that certainly would render instantaneously nonequivalent the closer pair of cis hydrogens of ethylene.

Reactions of Ethylene Complexes with Carbon Monoxide. All of the ethylene complexes readily react in THF with carbon monoxide at atmospheric pressure and room temperature. With the exception of the chloride derivative **1**, which is converted to the known carbonyl [(triphos)RhCl(CO)],[22] the ethylene compounds **2–5** add as many as two CO molecules to give acyl carbonyls of formula [(triphos)Rh(COR)(CO)] (R = CH_3 (**6**), C_2H_5 (**7**), C_6H_5 (**8**)). The addition of two CO molecules per molecule of metal complex is clearly demonstrated by the IR spectra, which contain absorptions both in the terminal carbonyl region and in the ν(C=O) region (ν(C≡O), ν(C=O): 1897, 1600 cm^{-1}, **6**; 1890, 1630 cm^{-1}, **7**; 1905, 1600 cm^{-1}, **8**). The ^1H NMR spectra are similar to each other except in the regions in which the protons of the different acyl functionalities resonate. Thus, a singlet at 2.13 ppm is attributed to the acetyl CH_3 while a triplet and a quartet at 1.13 and 2.53 ppm (J(HH) = 7.2 Hz), respectivley, are assigned to the propionyl C_2H_5 group. Finally, the phenyl protons of the benzoyl ligand can be identified as an AA′BB′C pattern in the region 7.6–6.8 ppm. All of the compounds are fluxional on the NMR time scale in ambient-temperature solutions as shown by the $^{31}P\{^1H\}$ NMR spectra, which invariably exhibit a single resonance for the three phosphorus atoms of triphos. As is observed quite frequently for five-coordinate triphos complexes, the present compounds are stereochemically rigid at low temperature.[9] In particular, the spectra at −90 °C consist of a doublet of triplets and a doublet of doublets (AM_2X spin system). In all cases, the J(PRh) value in the high-temperature limit is equal to the weighted average of the low-temperature-limit coupling constants, thus indicating that the only two phosphorus environments are just the two sites observed at low temperature.[23] A fast non-bond-breaking interconversion between trigonal-bipyramidal and square-pyramidal structures is believed to be responsible for the fluxionality of five-coordinate triphos complexes; which of the two geometries constitutes the ground state is a matter that depends on many factors, particularly on the nature of the two coligands.[9,12] As far as the present acyl carbonyls are concerned, the spectroscopic parameters are clearly consistent with trigonal-bipyramidal structures;[24] in particular, the CO ligand is assigned to an equatorial site because of the better back-bonding in that position.[25]

The acyl carbonyl complexes **6–8** are quite stable in the solid state but decompose very slowly in solution under an N_2 or Ar atmosphere with CO evolution. The propionyl complex is the least stable of the three. A sample of 30 mg in 3 mL of THF completely decomposes in the NMR tube on standing overnight under a nitrogen atmosphere at 20 °C, to give the known hydride carbonyl [(triphos)-RhH(CO)] (20%),[11] the new ethyl carbonyl [(triphos)Rh-(C_2H_5)(CO)] (**9**; 5%), and other unidentified phosphorus-containing products (yields based on NMR integration). Under the same conditions, 15% of the acetyl **6** transforms into the σ-methyl complex [(triphos)Rh-(CH_3)(CO)] (**10**).[26] This result is not new, as is has been already reported by Baird and Johnston that **6**, prepared by a different route, converts reversibly to **10**. However, no information was provided either on the amount of converted product or on the time required to accomplish the conversion. The benzoyl complex **8** is considerably more stable in deoxygenated solutions, since its conversion into the σ-phenyl derivative [(triphos)Rh(C_6H_5)(CO)] (**11**) is very slow (5% over 12 h).

The σ-ethyl and phenyl derivatives **9** and **11** are synthesized in moderate yields as pale orange crystals by the reaction of [(triphos)RhCl(CO)] in THF with EtMgBr or LiPh, respectively. The absence of functionalized CO in both compounds is clearly shown by the IR spectra, which contain no ν(C=O) signals. In contrast, a strong absorption due to a terminal CO ligand is present in both spectra, almost in the same positions found for the CO ligands in the parent acyl compounds (1888 and 1915 cm^{-1} for **9** and **11**). The ^1H NMR spectra show complicated resonances in the proper regions of σ-bonded ethyl and phenyl ligands in **9** and **11**, respectively, which have been simulated as $A_3B_2M_3X$ and AA′BB′CX spin systems. Like the parent acyl compounds, the σ-organyl complexes **9–11** are fluxional on the NMR time scale at room temperature and become stereochemically rigid at low temperature. In the slow-exchange limit, the $^{31}P\{^1H\}$ NMR spectra consist of AM_2X patterns which define the solution-state structure as trigonal bipyramidal for all of the compounds.[1i,12]

Also in good agreement with the chemical behavior of **10**, the ethyl and phenyl derivatives readily add CO, forming the corresponding σ-acyl complexes. The reactions are very fast, being completed in a few minutes.

(22) Siegl, W. O.; Lapporte, S. J.; Collmann, J. P. *Inorg. Chem.* **1971**, *10*, 2158.

(23) Woods, J. S. *Prog. Inorg. Chem.* **1972**, *16*, 227.
(24) DuBois, D. L.; Meek, D. W. *Inorg. Chem.* **1976**, *15*, 3076.
(25) Rossi, A. R.; Hoffmann, R. *Inorg. Chem.* **1975**, *14*, 365.
(26) Johnston, G. G.; Baird, M. C. *J. Organomet. Chem.* **1986**, *314*, C51.

In light of the experimental evidence herein presented, the carbonylation reactions of the ethylene complexes **1–5** appear reasonably clear. Carbon monoxide can simply displace the C_2H_4 ligand, as occurs in the reaction with **1**, or can promote migration of hydrogen from metal to ethylene, as is the case in the reaction with the hydride **2**. Replacement of C_2H_4 with a CO molecule is also the first step of the reactions with **3–5**. As a result, the σ-organyl carbonyls **9–11** should form. These, however, readily insert a CO molecule across the Rh–C bonds to give the stable σ-acyl carbonyls. As a matter of fact, monitoring the reactions of the ethylene complexes **2–5** by solution IR spectroscopy reveals that the addition of a second CO molecule to the σ-organyl carbonyls is even faster than ethylene displacement by CO. It is therefore reasonable to conclude that the σ-acyl complexes are the kinetic products of the carbonylation reactions.

As far as the mechanism of the CO insertion reactions is concerned, we have not purposefully carried out any detailed investigation because of the close analogy existing between the present reactions and those recently studied for a family of strictly related rhodium complexes with the polyphosphine PP_3, $P(CH_2CH_2PPh_2)_3$.[1d] In particular, it has been demonstrated that CO insertion across the Rh–C bonds in the trigonal-bipyramidal complexes $[(PP_3)RhR]$ ($R = CH_3$, C_6H_5), to give σ-acyls, occurs via an organyl carbonyl intermediate in which a phosphine arm of PP_3 is free. Accordingly, although phosphine and CO ligands are quite different, the mechanism shown in Scheme III can reasonably be extended also to the present reactions.

Reactions of Ethylene, σ-Organyl, and Acyl Complexes with Dihydrogen. The reaction of the chloride ethylene complex **1** with excess H_2 (1 atm, 20 °C) in THF results in the formation of beige microcrystals of $[(triphos)Rh(H)_2Cl]$ (**12**). This reaction is accompanied by the liberation of C_2H_6 and traces of C_2H_4. Compound **12** is fairly stable in the solid state and in deoxygenated solutions, in which it behaves as a nonelectrolyte. A medium-intensity, broad band at 1960 cm^{-1} is assigned to the rhodium–hydride stretch. The ^1H NMR spectrum in the hydride region exhibits a deceptively simple resonance that appears as a doublet of doublets of doublets centered at −7.35 ppm. In reality, this portion of the spectrum is slightly second order and can be properly simulated as the X part of an AA′XX′MZ spin system by using the following parameters: $\delta(H_X) = \delta(H_{X'}) = -7.35$ ppm; $J(P_AH_X) = J(P_{A'}H_{X'}) = 190.1$ Hz, $J(P_{A'}H_X) = J(P_AH_{X'}) = -6.0$ Hz, $J(P_MH_X) = J(P_MH_{X'}) = 9.8$ Hz, $J(H_XH_{X'}) = 4.9$ Hz, $J(P_AP_{A'}) = 19.8$ Hz, $J(H_XRh) = J(H_{X'}Rh) = 8.0$ Hz, $J(P_AP_M) = J(P_{A'}P_M) = 24.2$ Hz. ^{31}P decoupling experiments confirm the correctness of the $J(H_XRh)$ value. The $^{31}P\{^1H\}$ NMR spectrum consists of a first-order AM_2X spin system in which the doublet of doublets appears at higher field than the doublet of triplets. On the basis of all of these spectroscopic data, **12** is assigned an octahedral geometry in which the two hydride ligands are located mutually cis (Scheme I).

Under the same conditions, treatment of all of the other ethylene complexes with excess H_2 invariably results in the formation of the trihydride $[(triphos)Rh(H)_3]$[11a] (**13**) and the quantitative liberation of the corresponding hydrocarbon (C_2H_6, CH_4, or C_6H_6).

The reactions of the σ-organyl carbonyls **9–11** and the σ-acyl carbonyls **6–8** with H_2 in THF proceed in a manner essentially similar to that exhibited by the ethylene compounds, with the difference that the hydrogenolysis now requires reflux temperature (Scheme II). The final metal product of all reactions is the hydride carbonyl $[(triphos)RhH(CO)]$ (**14**), while the hydrogenolysis products are hydrocarbons for the σ-organyl complexes and aldehydes for the σ-acyls.

Scheme I

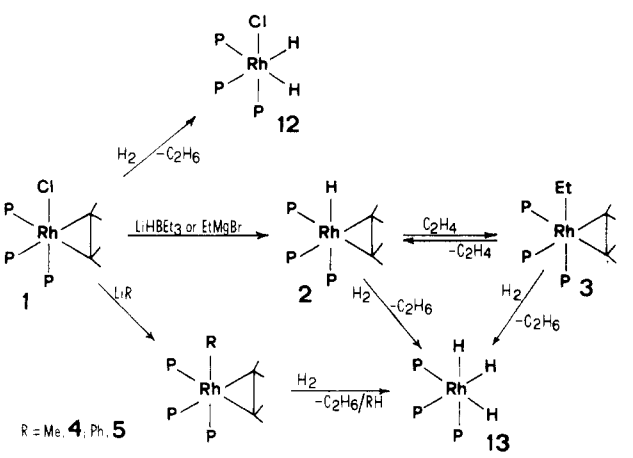

Scheme II

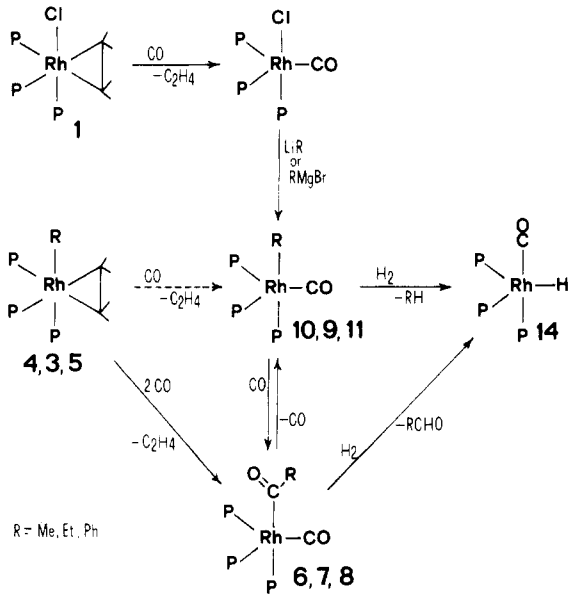

Scheme III

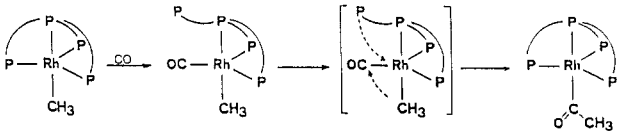

Synthesis and Characterization of the η^2-Alkyne Complex [(triphos)Rh(η^2-DMAD)]BPh_4 (DMAD = Dimethyl Acetylenedicarboxylate). Reactions with H_2, C_2H_4, and CO. The reaction of the chloride ethylene complex **1** in CH_2Cl_2/ethanol with DMAD, with $NaBPh_4$ as the halogen scavenger, yields $[(triphos)Rh(\eta^2\text{-DMAD})]BPh_4$ (**15**; Scheme IV). Compound **15** is quite stable in the solid state and in deoxygenated solutions, in which it behaves as a 1:1 electrolyte. The IR spectrum contains a strong absorption at 1750 cm^{-1}, which is consistent with the presence of a four-electron-donor π-alkyne ligand (metallacyclopropane type structure).[27] A strong band due to the ester ν(C=O) stretch is exhibited at 1680

(27) (a) Collmann, J. P.; Hegedus, L. S. *Principle and Applications of Organotransition Metal Chemistry*; University Science Books: Mill Valley, CA, 1980. (b) Rosenthal, U.; Schultz, W. *J. Organomet. Chem.* **1987**, *105*, 4462. (c) Capelle, B.; Dartiguenave, M.; Dartiguenave, Y.; Beauchamp, A. L. *J. Am. Chem. Soc.* **1983**, *105*, 4462.

Scheme IV

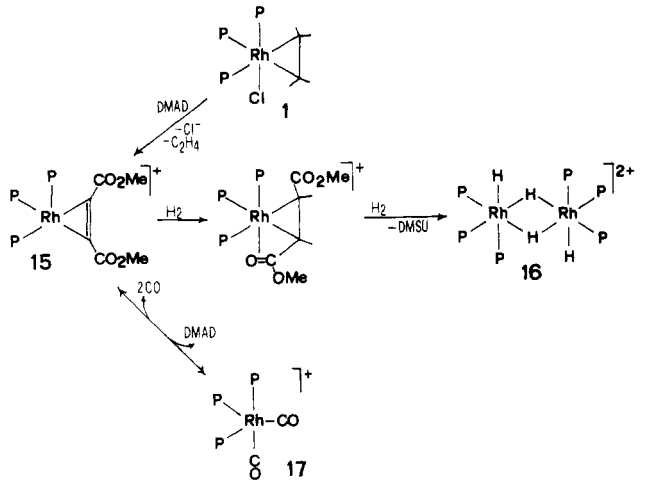

Scheme V

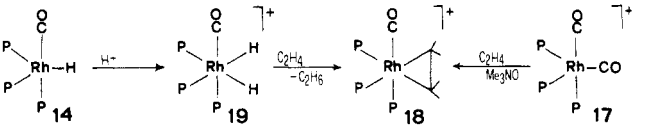

cm^{-1}, while ν(C—O—C) is found at 1220 cm^{-1}. The $^{31}P\{^1H\}$ NMR spectrum in CH_2Cl_2 consists of a single resonance (J(PRh) = 109.3 Hz), which exhibits only a slight temperature dependence of the chemical shift, from 39.85 ppm at +30 °C to 43.85 ppm at −100 °C. This behavior is typical of five-coordinate complexes of triphos containing η^2-bonded coligands.[9,10] The fluxionality is ascribed to a fast interconversion between trigonal-bipyramidal and square-pyramidal structures separated by a very low activation energy. It is worth noticing that, in these cases, the solid-state structure, as determined by X-ray methods, is generally square pyramidal.[10] The high fluxionality of **15** is shown also by the ^1H NMR spectrum, which displays a unique resonance (δ 4.01, CD_3COCD_3, 293 K) for the two OCH_3 groups. A unique resonance is found also for the two acetylenic carbons at 205.5 ppm, which provides further support for the metallacyclopropane structure.[27,28]

Compound **15** reacts with 1 atm of H_2 in THF at room temperature, quantitatively forming dimethyl succinate (DMSU) and the known dimer [(triphos)RhH(μ-H)$_2$HRh(triphos)](BPh$_4$)$_2$ (**16**).[2e] Monitoring the reaction by GC does not show the presence of free dimethyl maleate (DMMA) or dimethyl fumarate (DMFU) in the reaction mixtures, in keeping with the facile and rapid hydrogenation (1 atm of H_2, 20 °C) of the isolable intermediates [(triphos)Rh(π-DMMA)]BPh$_4$ and [(triphos)Rh(π-DMFU)]BPh$_4$ to **16** and DMSU.[2e] We therefore conclude that the sequence shown in Scheme IV well accounts for the hydrogenolysis reaction of **15**.

Treatment of **15** in THF with 1 atm of CO at room temperature results in the formation of [(triphos)Rh(CO)$_2$]BPh$_4$ (**17**)[22] via displacement of the alkyne by two CO molecules. This reaction is reversible and is controlled by the prevailing substrate; i.e., addition of excess DMAD to a THF solution of **17** quantitatively re-forms **15**. No reaction between **15** and C_2H_4 is observed even in refluxing THF and for long times. In contrast, the dicarbonyl **17** in THF reacts with C_2H_4, in the presence of Me_3NO as a CO scavenger, to give the novel carbonyl ethylene complex [(triphos)Rh(CO)(C_2H_4)]BPh$_4$ (**18**; Scheme V). The formation of **18** is invariably accompanied by that of [{(OPPh$_2$CH$_2$)C(CH$_3$)(CH$_2$PPh$_2$)$_2$}Rh(CO)$_2$]BPh$_4$ (yield ca. 40%) because of the competitive oxidation of a phosphine arm of triphos by Me_3NO. In this respect, it is worth noticing that some aspects of the solution chemistry of **17** have been previously interpreted in terms of an equilibrium between a five- and a four-coordinate species, the latter one containing a bidentate triphos ligand.[22,29]

Pure complex **18** is prepared as yellow crystals by protonation of the hydride carbonyl **14** in THF with a strong acid under an ethylene atmosphere, followed by NaBPh$_4$ addition. The reacton involves oxidative addition of the proton to give the dihydride [(triphos)Rh(H)$_2$(CO)]$^+$ (see below), which, successively, reacts with C_2H_4, yielding **18** and ethane. Compound **18** is fairly stable under inert atmospheres, but for a long storage in solution, C_2H_4 is preferred over N_2 or Ar. The IR spectrum contains ν(C≡O) at 2055 cm^{-1}, which is somewhat higher than ν(C≡O) in all of the other rhodium carbonyls herein reported. This may be taken as an indication for a different coordination site of CO on the coordination polyhedron, which seems to also be octahedral for **18** (see below). The compound is fluxional on the NMR time scale in ambient-temperature solutions, as shown by the $^{31}P\{^1H\}$ NMR spectrum, which consists of a doublet at 9.2 ppm (J(PRh) = 101.1 Hz) that becomes a broad, unresolved signal with $\omega_{1/2}$ = 300 Hz at 20 °C. Analogously to the acyl carbonyls **6**–**8**, compound **18** is stereochemically rigid at low temperature (the coalescence temperature is at ca. −15 °C). At −90 °C, the spectrum shows an AM$_2$X spin system with $\delta(P_A)$ = 24.38 ppm ($J(P_ARh)$ = 86.4 Hz, $J(P_AP_M)$ = 43.9 Hz) and $\delta(P_M)$ = 2.5 ppm ($J(P_MRh)$ = 108.0 Hz). The fluxionality of the complex cation is also evidenced by the ^1H NMR spectrum, in which the ethylene protons constitute a clean AA′BB′ pattern with J(AB) + J(AB′) = 10.3 Hz only below −20 °C. At higher temperatures the resonance is significantly broadened. As observed for **1**, the spin system does not change on lowering the temperature, the only variation being an upfield shift of the AA′ portion from 2.1 (20 °C) to 1.8 ppm (−85 °C). The $^{13}C\{^1H\}$ NMR spectrum (CD_3COCD_3, 20 C) shows a unique resonance at 37.5 ppm for the ethylene carbons. On the basis of all these data, **18** is assigned a ground-state structure essentially similar to that of **1**; i.e., the C_2H_4 molecule lies in the equatorial plane of an octahedron in which CO is located trans to the apical phosphorus.

When **14** in THF is protonated by $HOSO_2CF_3$ under an argon or nitrogen atmosphere, the dihydride carbonyl [(triphos)Rh(H)$_2$(CO)]BPh$_4$ (**19**) is quantitatively obtained as colorless crystals after the addition of NaBPH$_4$ in ethanol. The compound is fairly stable in the solid state and in deoxygenated solutions, in which it behaves as a 1:1 electrolyte. The spectroscopic properties of **19** closely resemble those found for the dihydide chloride **12**. The ν(Rh—H) and ν(C≡O) stretching frequencies are now at 1962 and 2066 cm^{-1}, respectively. The $^{31}P\{^1H\}$ NMR spectrum consists of a first-order, temperature-invariant AM$_2$X spin system, as expected for an octahedral structure essentially similar to that proposed for **12** (Scheme V). The two mutually cis hydride ligands give rise to a second-order NMR resonance centered at −7.24 ppm, which has been properly simulated as the X part of an AA′MXX′Z spin system by using the following parameters: $J(P_AH_X)$ = $J(P_{A'}H_{X'})$ = 140.0 Hz, $J(P_AH_X)$ = $J(P_AH_{X'})$ = −5.2 Hz, $J(P_MH_X)$ = $J(P_MH_{X'})$ = 3.2 Hz, $J(H_XH_{X'})$ = 6.7 Hz, J-

(28) Shur, V. B.; Burlakov, V. V.; Vol'pin, M. E. *J. Organomet. Chem.* **1988**, *347*, 77.

(29) Behrens, H.; Ellermann, J.; Hoenberger, E. F. *Z. Naturforsch.* **1980**, *35B*, 661.

Table IV. Hydrogenation of 1-Hexene[a]

catalyst	temp, °C	pressure of H_2 atm	conversn, %	crude composition, %			
				n-hexane	*trans*-2-hexene	*cis*-2-hexene	1-hexene
A	20	1	90.1	66.0	15.0	9.1	9.9
B	20	1	93.6	78.9	10	4.7	6.4
C[c]	20	1	58.1	25.5	16.2	15.6	41.9
A[b]	20	1	100	55.0	23.2	21.8	
D[b]	20	1	2.0	1.0	0.5	0.5	98.0
A	20	30	99.6	99.6			0.4
B	20	30	95.9	94.9	1.0		4.1
C	20	30	95.3	95.3			4.7
A	60	30	100	100			
B	60	30	100	100			
C	60	30	100	100			
D[b]	100	30	100	100			

[a] Reaction conditions: 2 mmol of 1-hexene, 0.02 mmol of catalyst, 25 mL of THF, reaction time 3 h. Catalyst C = [(triphos)RhH(CO)]; catalyst D = [(triphos)RhCl(C_2H_4)]. [b] 2 mmol of 1-hexene, 0.2 mmol of catalyst. [c] *trans*-3-Hexane (0.6%) and *cis*-3-hexene (0.2%) are also present.

Table V. Hydrogenation of *cis*-Stilbene[a]

catalyst	temp, °C	conversn, %	crude composition, %		
			1,2-diphenylethane	*trans*-stilbene	*cis*-stilbene
A	20	99.6	23.8	75.8	0.4
B	20	65.9	0.3	65.6	34.1
A	60	99.6	39.2	60.4	0.4
B	60	98.4	1.7	96.7	1.6

[a] Reaction conditions: 2 mmol of *cis*-stilbene, 0.02 mmol of catalyst, 25 mL of THF, hydrogen pressure 1 atm, reaction time 3 h.

$(P_AP_{A'})$ = 21.6 Hz, $J(H_XRh) = J(H_{X'}Rh)$ = 15.2 Hz, $J(P_AP_M) = J(P_{A'}P_M)$ = 34.9 Hz. Also, it is possible to conclude that $J(HP_A)$ is much smaller in **19** than in the closely related chloride derivative **12**, most likely because of the stronger trans influence of CO vs that of Cl.

Provided that the phosphorus–rhodium coupling constants can be taken as a measure of the trans influence,[15,30] a perusal of the $J(P_ARh)$ values within the present family of octahedral ethylene complexes reveals that the trans influence of the apical ligands is in the order Ph > Et > Me > H > CO ≫ Cl. With the exception of the phenyl group, this order is in agreement with several series of trans-influence ligands that have been obtained by other methods.[31] Although limited to two compounds only, the same order is found for the dihydrides **12** and **19**.

Homogeneous Hydrogenation and Hydroformylation Reactions of Olefins. Surveying the various types of reactions reported in the previous sections, one may readily infer that organorhodium complexes of triphos have promise in the hydrogenation and hydroformylation reactions of olefins. Furthermore, it is quite evident that many of the complexes described are potential precursors to two catalyst systems, the [(triphos)RhH] and [(triphos)Rh]$^+$ fragments. They differ from each other only in a hydride ligand, but as will be shown below, this makes a great difference.

Hydrogenation Reactions. Both the alkyne complex **15** and the ethylene complexes **2–5** are active catalyst precursors for the hydrogenation of alkenes and alkynes at 20 °C and 1 atm of H_2. Tables IV–VII summarize the results obtained for a variety of substrates in THF solutions and for a reaction time of 3 h. As far as the ethylene complexes are concerned, the active catalyst species appears to be the 16-electron fragment [(triphos)RhH] (catalyst A). In contrast, the naked 14-electron system

Scheme VI

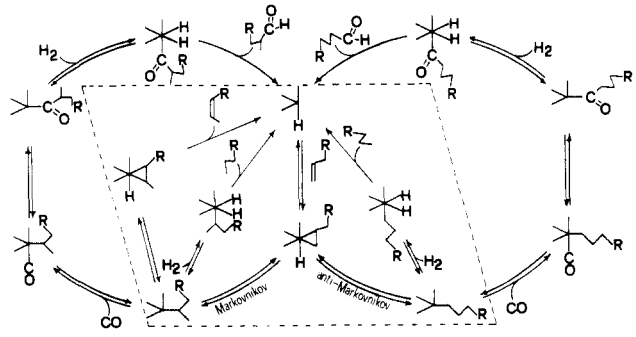

[(triphos)Rh]$^+$ (catalyst B) is considered the catalyst for the hydrogenation reactions assisted by **15**.

A perusal of the data reported in Table IV reveals that, at 20 °C and 1 atm of H_2, catalyst B is only slightly more active than catalyst A for the conversion of 1-hexene but appreciably more efficient for the hydrogenation to hexane. Increasing the catalyst to substrate ratio increases both the total conversion and the amount of isomerized olefin. As expected, the amount of 2-hexene (cis and trans) in the crude mixture decreases on increasing the pressure of H_2 (at 30 atm of H_2, hydrogenation proceeds quantitatively for both catalyst systems). The termination products are the trihydride **13** (catalyst A) and the $(\mu\text{-H})_2$ dimer **16** (catalyst B).

In view of the experimental results presented in the previous sections as well as the large amount of data on homogeneous hydrogenations reported in the literature,[32] there is little doubt that the inner cycles in the dashed box shown in Scheme VI (catalyst A) and Scheme VII (catalyst B) can correctly describe the present catalytic reactions (the precycles relating to hydrogenation of C_2H_4 and DMAD have been omitted for clarity). It is worth noticing that while catalyst A involves a sequence of 16- and 18-electron species, catalyst B involves a sequence of 14-, 16-, and 18-electron species. In both cases, no phosphine dissociation is necessary to accomplish the hydrogenation reactions. The major effectiveness of catalyst A for the isomerization of 1-hexene to 2-hexene may be related to the different nature of the σ-alkyl intermediates in the two catalytic cycles. In effect, the alkyl intermediate in Scheme VI appears more propitious to β-H elimination, as it is very

(30) Meek, D. W.; Mazanek, T. J. *Acc. Chem. Res.* **1981**, *14*, 266.
(31) Appleton, T. G.; Clark, H. C.; Manzer, L. E. *Coord. Chem. Rev.* **1973**, *10*, 335.

(32) (a) James, B. R. *Homogeneous Hydrogenation*; Wiley: New York, 1973. (b) James, B. R. *Adv. Organomet. Chem.* **1979**, *17*, 319. (c) Kieborn, A. P. G.; van Rantwijk, F. *Hydrogenation and Hydrogenolysis in Synthetic Organic Chemistry*; Delft University Press: Delft, The Netherlands, 1979.

Table VI. Hydrogenation of Diphenylacetylene[a]

catalyst	temp, °C	conversn, %	crude composition, %			
			1,2-diphenylethane	*trans*-stilbene	*cis*-stilbene	diphenylacetylene
A	20	96.4	5.5	63.7	27.2	3.6
B	20	19.3	0.3	15.1	3.9	80.7
A	20[b]	100	72.7	27.1	0.2	
B	20[b]	45.3	1.0	35.7	8.6	54.7
A	60	99.9	13.0	85.2	1.7	0.1
B	60	70.6	1.8	45.9	22.9	29.4
A	60[b]	100	100			
B	60[b]	100	85.6	14.4		
B	100[b]	100	100			

[a] Reaction conditions: 2 mmol of diphenylacetylene, 0.02 mmol of catalyst, 25 mL, THF, hydrogen pressure 1 atm, reaction time 3 h. [b] Hydrogen pressure 30 atm.

Table VII. Hydrogenation of Dimethyl Acetylenedicarboxylate[a]

catalyst	conversn, %	crude composition, %			
		succinate	maleate	fumarate	acetylene
A	87.3	25.0	6.3	56.0	12.7
B	92.9	13.6	60.3	19.0	7.1

[a] Reaction conditions: 2 mmol of dimethyl acetylenedicarboxylate, 0.02 mmol of catalyst, 25 mL of THF, hydrogen pressure 1 atm, temperature 60 °C, reaction time 3 h.

Scheme VII

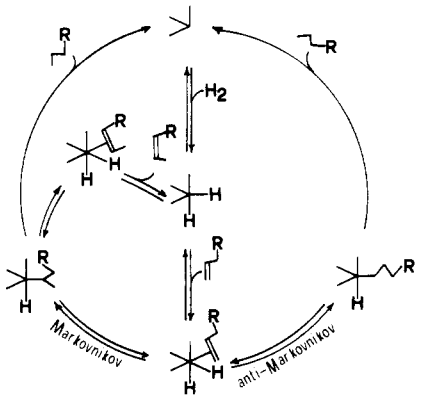

open at the metal. In contrast, the alkyl intermediate in Scheme VII is more crowded and, therefore, the reductive elimination of the alkane may prevail over β-H elimination. By use of the same steric argument, the Markovnikov addition of hydride to coordinated alkene, which is responsible for the double-bond isomerization, appears to be facilitated for catalyst A.[33,34]

The much lower efficiency of the chloride ethylene complex 1 to function as a hydrogenation catalyst of 1-hexene (Table IV) is a direct consequence of its difficulty in forming catalyst A. In fact, the formation of the fragment [(triphos)RhH] requires the reductive elimination of HCl, a process that does not occur at low pressures of H_2.

There is not much of a difference between catalysts A and B as far as the hydrogenation reactions of 1-hexene are concerned. In contrast, the two systems exhibit quite different behaviors when the alkene bears bulky, electron-withdrawing substituents as in the case of *cis*-stilbene (Table V). Catalyst A is now much more active than catalyst B, effecting an almost quantitative conversion of the *cis*-alkene to 1,2-diphenylethane (23.8%) and to *trans*-tilbene (75.8%) at room temperature and 1 atm of H_2. Under the same conditions, only partial isomerization to the trans olefin (65.6%) is effected by catalyst B. The different behavior of the two systems becomes more evident at high temperature: at 60 °C, *cis*-stilbene is quantitatively converted by both catalysts but only catalyst A proves able to hydrogenate the alkene. A reasonable explanation for the diverging behavior of these systems is provided by taking into account the electronic properties of the two metal fragments and of the alkene as well. In particular, the minor activity of the 14-electron system is certainly a consequence of its inability, compared to the 16-electron catalyst A, to form a stable adduct with an activated alkene such as *cis*-stilbene. However, this does not explain why catalyst B at low hydrogen pressures does not hydrogenate the olefin, which, on the other hand, is rapidly isomerized, especially at high temperature. In other words, there is no apparent reason why a complicated process involving the rotaton of the bulky 1,2-diphenylethyl ligand around the C–C single bond and successive β-H elimintion should prevail over alkane elimination. Indeed, the isomerization does not proceed through a hydride migraton/β-elimination mechanism. We have found that system B catalytically isomerizes *cis*-stilbene to *trans*-stilbene in THF solution without requiring the assistance of H_2 or of any other hydridic or protonic species. This phenomenon is not new for tripodal polyphosphine metal systems.[2b] Preliminary theoretical studies suggest that the cis–trans isomerizaton occurs through a polarization effect of the metal over the olefin.[35] The rate of isomerization increases with the temperature and is not influenced by the presence of H_2. Only at high pressures of hydrogen (see Table VI) does catayst B promote the hydrogenation of *cis*-stilbene to 1,2-diphenylethane, thus suggesting that the rate-determining step of the catalytic cycle is the addition of H_2 to the (triphos)Rh(alkene) intermediate.

The diverging behaviors of catalysts A and B become even more evident when the substrate for hydrogenation is a disubstituted alkyne such as diphenylacetylene (Table VI) or DMAD (Table VII). At 1 atm of H_2 and 20 °C, diphenylacetylene is quantitatively reduced in the presence of catalyst A to a mixture of 1,2-diphenylethane, *trans*-stilbene, and *cis*-stilbene. Monitoring the hydrogenation reactions by GC shows that the alkyne displaces the olefin from the metal after the isomerization of the *cis*-alkene and before the hydrogenation to alkane; only at very low concentrations of alkyne does hydrogenation of *trans*-stiblene take place. Increasing the temperature produces as the predominant product *trans*-stilbene (at 60 °C,

(33) (a) Bird, C. W. *Transition Metal Intermediates in Organic Synthesis*; Academic Press: New York, 1968. (b) Tsuti, M.; Courtney, A. *Adv. Organomet. Chem.* **1977**, *17*, 241.

(34) (a) Evans, D.; Osborn, J. A.; Wilkinson, G. *J. Chem. Soc. A* **1968**, 3133. (b) Masters, C. *Homogeneous Transition Metal Catalysis*; Chapman and Hall: London, 1981. (c) Markó, L. In *Aspects of Homogeneous Catalysis*; Ugo, R., Ed.; Reidel: Dordrecht, The Netherlands, 1974; Vol. 2, Chapter 1.

(35) Bianchini, C.; Mealli, C.; Meli, A. Manuscript in preparation.

Table VIII. 1-Hexene Hydroformylation in the Presence of [(triphos)RhH(C_2H_4)][a]

	aldehydes					olefins				
		composition, %			hexane	resid composition, %				
temp, °C	yield, %	HEP	2MH	2EP	yield, %	A	*trans*-B	*cis*-B	*trans*-C	*cis*-C
20						100				
40	17.2	55.4	44.6			97.0	3.0	trace		
60	55.8	60.8	39.2			62.6	24.7	9.8	2.3	0.6
60[b]	6.3	81.4	18.6			100				
80	78.4	48.5	40.4	11.1	1.1	4.2	58.1	18.2	15.8	3.7
80[c]	70.6	48.0	41.1	10.9	3.9	7.7	53.3	19.0	17.7	2.3
100	99.0	45.0	42.0	13.0	0.2	6.7	53.6	16.6	22.3	0.8
100[b]	69.2	83.9	16.1		5.0	38.0	15.2	39.2	7.5	

[a] Reaction conditions: 2 mmol of 1-hexene, 0.02 mmol of catalyst, 25 mL of THF, hydrogen pressure 15 atm, carbon monoxide pressure 15 atm, reaction time 3 h. Abbreviations: HEP, heptanal; 2MH, 2-methylhexanal; 2EP, 2-ethylpentanal; A, 1-hexene; B, 2-hexene; C, 3-hexene. [b] 2 mmol of 1-hexene, 0.2 mmol of catalyst. [c] Catalyst precursor [(triphos)Rh(CO)H].

trans-stilbene is 85% of the converted alkyne), while at a high hydrogen pressure, the alkane is quantitatively formed. In accord with the results found for *cis*-stilbene, no appreciable production of alkane is observed in the hydrogenation of diphenylacetylene with catalyst B unless a high pressure of H_2 is used. The conversion of acetylene to alkane proceeds much more slowly with catalyst B, which predominantly promotes the formaton of the trans isomer. The lower activity of catalyst B vs that of A is again attributed to the different nature of the intermediate species, i.e. [(triphos)Rh(alkyne)]$^+$ and [(triphos)RhH(alkyne)], which are expected to oxidatively add H_2.

The crucial role of the alkyne substituents in determining the course of the hydrogenation reactions with either catalyst A or catalyst B is clearly shown by the DMAD and DMMA cases. Interestingly, system A now proves more active than system B for the isomerization of the *cis*-alkene. In particular, the isomerization to fumarate proceeds twice as fast as hydrogenation to succinate. In good agreement with our previous results, we have found that system A is a very active catalyst for the isomerization of dialkyl maleates to dialkyl fumarates in the absence of hydrogen. The termination products of the isomerization catalytic cycle are the hydride fumarate complexes [(triphos)RhH(η^2-dialkyl fumarate)] (R = Me, Et).[2h] Once again, the different behavior of the two catalyst systems is related to the stability of the η^2-alkene intermediate. The [(triphos)Rh]$^+$ fragment is now able to form very stable and isolable adducts with *cis*-alkenes because dialkyl maleates can coordinate rhodium through both the C=C double bond and the C=O ester group (Scheme IV).[2e] In this way, the complexes are coordinatively and electronically saturated and the cis olefin is blocked. Accordingly, both dihydrogen addition and alkene isomerization are not easily accessible. Noticeably, the reactions proceed without disturbing the CO_2Me groups.

In conclusion, the two hydrogenation catalysts A and B are extremely sensitive to both the electronic and steric nature of the olefin substituents. In particular the presence of substituents containing potential donor atoms that can provide the metal–alkene intermediates with additional stability (CO_2R) appears important in determining the course of the reactions.

When the σ-organyl carbonyls **9–11** or the σ-acyl carbonyls **6–8** are employed as catalyst precursors for the hydrogenation of alkenes, quite different results are obtained as compared to those found for **2–5** or **15**. In all cases, the termination product is the hydride carbonyl **14**, which most likely is the common catalyst. This system is much less active than catalysts A and B, the quantitative hydrogenaton of 1-hexene being obtained only at high pressures of H_2. Under standard conditions, ca. 50% conversion of alkene is produced with almost comparable rates of hydrogenation and isomerization (Table IV).

Hydroformylation Reactions. The [(triphos)RhH] Catalyst. Preliminary tests on the hydroformylation reactions of 1-hexene with the ethylene complexes **2–5**, the σ-organyl carbonyl **9–11**, or the σ-acyl carbonyls **6–8** as catalyst precursors showed that all of these compounds display almost identical activities as regards both the total conversion and the isomeric product composition. Accordingly, in order to study the hydroformylation reactions[34] of 1-hexene, we decided to use the ethylene hydride complex **2** as the catalyst precursor.

The system proves very active only at 100 °C, where 1-hexene is quantitatively converted to the aldehyde. Higher temperature runs are similar to the 100 °C run. Table VIII summarizes the results obtained and reveals that the terminal alkene is preferentially carbonylated over the isomerized 2-hexene. The reactions are not very selective with a catalyst–substrate ratio of 0.01, producing comparable amounts of linear and branched aldehydes. Interestingly, the normal–iso ratio increases appreciably on raising the catalyst to substrate ratio (for a catalyst–substrate ratio of 0.1, the normal–iso ratio is 5.2 while no 2-ethylpentanal is formed). The increase in selectivity is accompanied by a decrease in activity. In an attempt to understand why an increase in the catalyst concentration results in an increase of selectivity and a decrease in activity, we have studied the hydroformylation reactions of 1-hexene with the binuclear polyhydride complexes [(triphos)RhH(μ-H)$_2$HRh(triphos)] (**20**), [(triphos)RhH(μ-H)$_2$HRh(triphos)](BPh$_4$)$_2$ (**16**),[2e] and [(triphos)Rh(μ-H)$_3$(triphos)]BPh$_4$ (**21**).[14c] In fact, we were stimualted by the idea that a modification of the catalyst might have occurred at high concentrations due to the formation of metal aggregates or clusters. Since we knew that triphos is not appropriate to form complexes with high nuclearity because of its particular steric and geometric requirements, we focused our attention on the dimers, as they are quite numerous and important in the coordination chemistry of this tripodal ligand.[1a,13,14] Particular attention was devoted to complexes **16**, **20**, and **21** because they are strictly related to the [(triphos)RhH] moiety, which, most likely, is the catalyst system also for the hydroformylation reactions. As we have previously shown (Scheme I), the [(triphos)RhH] fragment can readily add molecular hydrogen to form the trihydride **13**, which, in turn, is known to give the dimer **20** by either thermal decomposition in THF or hydrogen transfer to an alkene (Scheme VIII).[2e] Both reactions have been interpreted as condensation reactions of a molecule of **13** with a [(triphos)RhH] fragment. The neutral dimer **20** is readily converted to **16** by chemical oxidation (it is enough to use atmospheric oxygen), while **16** converts to **21** by simply standing in THF solution.[2e]

Table IX. 1-Hexene Hydroformylation in the Presence of Rhodium Dimers[a]

	aldehydes			olefins		
		composition, %		resid composition, %		
catalyst	yield, %	HEP	2MH	A	*trans*-B	*cis*-B
21	4.7	76.0	24.0	98.4	1.6	
16	6.9	70.2	29.8	99.0	1.0	
20[b]	28.5	69.8	30.2	60.3	29.1	10.6

[a] Reaction conditions: 2 mmol of 1-hexene, 0.02 mmol of catalyst, 25 mL of DMF, hydrogen pressure 15 atm, carbon monoxide pressure 15 atm, reaction time 3 h, temperature 80 °C. For abbreviations see footnote *a* of Table VIII. [b] 25 mL of THF.

Scheme VIII

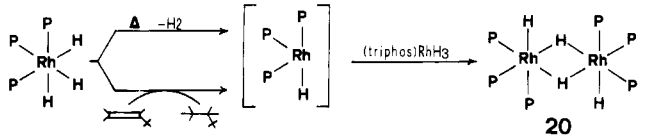

Some of the results that we have collected for the hydroformylation reactions of 1-hexene using as catalyst precursors **16**, **20**, and **21** are reported in Table IX (the data for **20** and **21** are given for *N*,*N*-dimethylformamide solutions, as the two dimers are not soluble in THF). Interestingly, both the total conversion of alkene to aldehyde and the product composition closely resemble those found for the hydroformylation reactions carried out with a catalyst–substrate ratio of 0.1. This provides support for our hypothesis that, at high concentrations, the catalyst may lose its original mononuclear nature to form binuclear species. A detailed investigation on the hydroformylation reactions, of **16**, **20**, and **21** and of related dimeric polyhydrides of rhodium is presently underway. As has already been reported for the catalytic hydrogenations of alkene and alkynes,[2e] the compounds appear to maintain the dimeric framework during the catalytic cycles. However, at the present stage, it is not possible to propose any definite catalysis cycle.

On the basis of the chemistry presented in Schemes I and II as well as the hydroformylation results, a reasonable catalysis cycle for the reactions with the catalyst–substrate ratio of 0.01 is shown in Scheme VI, in which the active catalyst species is again the 16-electron [(triphos)RhH] system. As is commonly accepted,[34] the rate-determining step might be the 16-electron four-coordinate σ-acyl intermediate, as we note that the reactions of the σ-organyl carbonyl complexes with H_2 to give the trihydride **13** require high temperatures.

A perusal of Scheme II suggests that an alternative catalyst precursor for the hydroformylation reaction might well be the hydride carbonyl **14**, which, recall, is the termination product of the catalysis cycle. Also, **14** has been previously employed as a catalyst for the hydroformylation of styrene with a mechanism involving the dissociation of a phosphine arm of triphos.[36] We have compared the behavior of **14** with that of **2**. The hydride **14** is ca. 10% less active than **2**, but the aldehyde product displays almost the same isomeric composition. Accordingly, this result does not allow one to exclude the participation of **14** in the hydroformylation reaction either in a secondary catalysis process (Scheme IX, outside loop) or as a precursor to catalyst A (Scheme IX, inside loop). In the latter eventuality, the minor activity of **14** might be due to an induction period.

(36) Ott, J. Dissertation, ETH No. 8000, Zurich, Switzerland, 1986.

Scheme IX

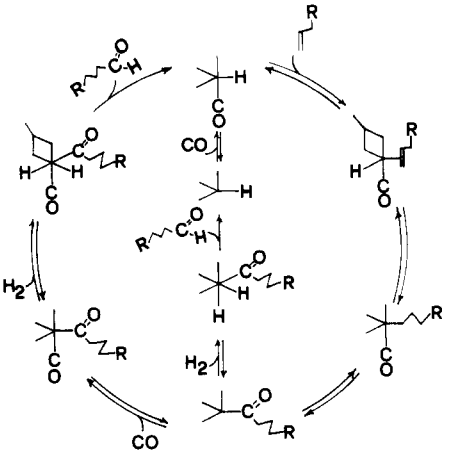

Scheme X

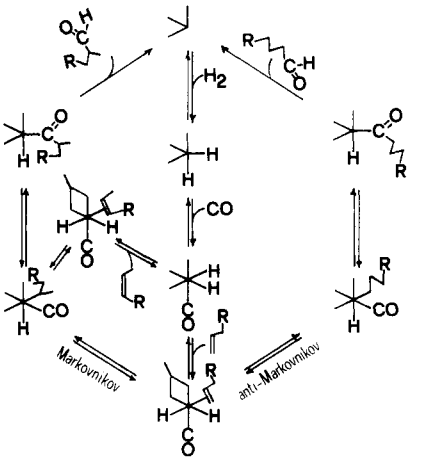

The [(triphos)Rh]$^+$ Catalyst. Table X summarizes the results of the hydroformylation of 1-hexene with the η^2-alkyne complex **15** as the catalyst precursor. Quite similar results have been observed for the ethylene carbonyl **18** and for the dihydride carbonyl **19**, therefore indicating that the active catalyst system is the common 14-electron fragment [(triphos)Rh]$^+$ (catalyst B). Catalyst B displays a completely different behavior as compared to the 16-electron catalyst A: it is much less active, and the selectivity to the linear aldehyde increases as the temperature increases. In addition the rate of hydroformylation increases on increasing the catalyst–substrate ratio but the selectivity to the linear aldehyde diminishes.

The minor efficiency of catalyst B as compared to that of catalyst A may be interpreted in terms of a dissociative mechanism.[34] In fact, the only reasonable catalysis cycles are those in which, at least on one occasion, triphos behaves as a bidentate ligand, unless one admits the intermediacy of oversaturated 20-electron species (Scheme X). Obviously, the rupture of a P–Rh bond belonging to a six-membered metalla ring requires some energy. It is worth mentioning that, for all of these catalyst systems, the hydrogenation of the olefin is inhibited by the presence of CO.

As a final consideration, we honestly state that all of the triphos catalysts herein presented are not as fast and selective as many other rhodium systems,[37] including the

(37) Hendriksen, D. E.; Oswald, A. A.; Ansell, G. B.; Leta, S.; Kastrup, R. V. *Organometallics* **1989**, *8*, 1153. Pruett, R. L. *Adv. Organomet. Chem.* **1979**, *17*, 1. Cornils, B. In *New Syntheses with Carbon Monoxide*; Falbe, J., Ed.; Springer-Verlag: West Berlin, 1980. Tkatchenko, I. In *Comprehensive Organometallic Chemistry*; Wilkinson, G., Stone, F. G. A., Abel, E. W., Eds.; Pergamon Press: Oxford, U.K., 1982; Vol 8, p 101.

Table X. 1-Hexene Hydroformylation in the Presence of [(triphos)Rh(DMAD)]BPh_4[a]

	aldehydes			olefins				
		composition, %		resid composition, %				
temp, °C	yield, %	HEP	2MH	A	*trans*-B	*cis*-B	*trans*-C	*cis*-C
20				100				
40	12.6	56.6	43.4	96.2	3.0	0.8		
60	20.2	63.5	36.5	80.1	14.2	5.7		
60[b]	24.8	60.7	39.3	97.0	3.0			
100	34.2	80.4	19.6	72.2	18.5	7.8	0.9	0.6
100[b]	60.9	71.1	28.9	2.8	63.3	29.3	4.5	0.1

[a] Reaction conditions: 2 mmol of 1-hexene, 0.02 mmol of catalyst, 25 mL of THF, hydrogen pressure 15 atm, carbon monoxide pressure 15 atm, reaction time 3 h. For abbreviations see footnote *a* of Table VIII. [b] 2 mmol of 1-hexene, 0.2 mmol of catalyst.

related $RhH(CO)(PPh_3)_3$ complex.[38] On the other hand, we wish to stress that the use of the triphos ligand allows the isolation and characterization of many intermediate species not normally seen in hydroformylation catalysis cycles. Studies are presently underway to evaluate the influence of the reaction conditions on the rates and isomeric compositions.

Experimental Section

General Information. All reactions and manipulations were routinely performed under nitrogen, except where otherwise stated, by using Schlenk-line techniques. Reagent grade chemicals were used in the preparations of the complexes. THF and CH_2Cl_2 were purified by distillation from $LiAlH_4$ and CaH_2 under nitrogen, respectively. All the other solvents were reagent grade and were used as received. Literature methods were used for the preparation of triphos[39] and $[RhCl(C_2H_4)_2]_2$.[40] The solid compounds were collected on sintered-glass frits and washed with appropriate solvents before being dried under a stream of nitrogen. Infrared spectra were recorded on a Perkin-Elmer 1600 Series FTIR spectrophotometer using samples mulled in Nujol between KBr plates. ^1H and $^{13}C\{^1H\}$ NMR spectra were recorded at 299.945 and 75.429 MHz, respectively, on a Varian VXR 300 spectrometer. Peak positions are relative to tetramethylsilane as an external reference (proton spectra) or are calibrated against the solvent (carbon spectra). $^{31}P\{^1H\}$ NMR spectra were recorded on Varian CFT 20 and Varian VXR 300 instruments operating at 32.19 and 121.42 MHz, respectively. Chemical shifts are relative to external 85% H_3PO_4, with downfield values reported as positive. Conductivities were measured with a WTW Model LBR/B conductivity bridge. The conductivity data were obtained at sample concentrations of ca. 10^{-3} M in nitroethane solutions. GC analyses were performed by using the following apparatus: Shimadzu GC-8A gas chromatograph coupled with a Shimdadzu C-R6A Chromatopac, Perkin-Elmer Sigma 1 system, or Perkin-Elmer 8320 capillary gas chromatograph. GC–MS spectra were collected by using a Hewlett-Packard Model 5970A chromatograph equipped with a mass detector.

Simulation of NMR spectra was achieved by using updated versions of the LAOCN4[41] and DAVINS programs.[42] The initial choices of shifts and coupling constants were refined by successive iterations, the assignment of the experimental lines being performed automatically. The final parameters gave a fit to the observed line positions of better than 0.3 Hz.

Preparation of [(triphos)RhCl(C_2H_4)] (1). Solid triphos (1.25 g, 2 mmol) was added to a solution of $[RhCl(C_2H_4)_2]_2$ (0.39 g, 1 mmol) in CH_2Cl_2 (20 mL) under ethylene. After 30 min ethanol (30 mL) was added and orange crystals began to form; the precipitation was completed by adding *n*-heptane (15 mL) to the mixture. The crystals were collected by filtration and washed with a 1:1 mixture of ethanol and *n*-heptane; yield 85%. Anal. Calcd for $C_{43}H_{43}ClP_3Rh$: C, 65.28; H, 5.48; Cl, 4.48; Rh, 13.01. Found: C, 65.01; H, 5.34; Cl, 4.51; Rh, 12.92.

Preparation of [(triphos)RhH(C_2H_4)] (2). A. $LiHBEt_3$ (1 M in THF, 2 mL, 2 mmol) was syringed into a stirred saturated solution of **1** (1 g, 1.26 mmol) in THF (20 mL) under ethylene. Within 20 min the starting solid dissolved, producing an orange solution. After ethylene was replaced with nitrogen, on addition of 1-butanol (30 mL) and partial evaporation of the solvent yellow crystals precipitated in 85% yield. They were filtered off and washed with ethanol and petroleum ether. Anal. Calcd for $C_{43}H_{44}P_3Rh$: C, 68.26; H, 5.86; Rh, 13.60. Found: C, 68.13; H, 5.81; Rh, 13.49. IR: 1965 cm^{-1} (ν(Rh—H)).

B. A stirred saturated solution of **1** (1 g, 1.26 mmol) in THF (20 mL) was treated with a solution of EtMgBr (2 M in THF, 1 mL, 2 mmol). Within 30 min the starting product dissolved and the resulting solution, eluted with 1-butanol (40 mL), gave yellow crystals, which were filtered off and washed as above; yield 72%.

C. A THF (30 mL) suspension of [(triphos)RhH_3] (0.73 g, 1 mmol) was refluxed for 2 h under ethylene. After ethylene was replaced with nitrogen, 1-butanol (30 mL) was added to the resulting red-orange solution. On concentration yellow crystals precipitated, which were filtered off and washed as above ; yield 65%.

Preparation of [(triphos)Rh(C_2H_5)(C_2H_4)] (3). A. A stirred saturated solution of **1** (1 g, 1.26 mmol) in THF (30 mL) under ethylene was treated with a solution of $LiHBEt_3$ (1 M in THF, 2 mL, 2 mmol) or EtMgBr (2 M in THF, 1 mL, 2 mmol). Within 30 min the starting product dissolved and the resulting solution was left standing for 2 h. Addition of 1-butanol (20 mL) and *n*-heptane (10 mL) gave a yellow microcrystalline solid in ca. 62% yield, which was filtered off and washed with a 1:1 mixture of ethanol and *n*-heptane and petroleum ether. Anal. Calcd for $C_{45}H_{48}P_3Rh$: C, 68.88; H, 6.17; Rh, 13.11. Found: C, 68.79; H, 6.17; Rh, 13.05.

B. After ethylene was bubbled into a THF (20 mL) solution of **2** (0.38 g, 0.5 mmol) for 2 h, addition of 1-butanol (20 mL) and *n*-heptane (10 mL) gave **3** in 85% yield. When a solution of **3** (0.39 g, 0.5 mmol) in THF (20 mL) under nitrogen was left standing for 2 h, compound **2** could be recovered almost quantitatively by adding 1-butanol (40 mL).

Preparation of [(triphos)Rh(CH_3)(C_2H_4)] (4). LiMe (1.6 M in THF, 3 mL, 4.8 mmol) was syringed into a stirred saturated solution of **1** (1 g, 1.26 mmol) in THF (50 mL) under ethylene. Within 1 h the starting solid dissolved, producing an orange solution. After ethylene was replaced with nitrogen, on addition of ethanol (30 mL) and partial evaporation of the solvent yellow crystals precipitated in 75% yield. They were filtered off and washed with ethanol and petroleum ether. Anal. Calcd for $C_{44}H_{46}P_3Rh$: C, 68.57; H, 6.02; Rh, 13.35. Found: C, 68.53; H, 5.99; Rh, 13.28.

Reaction of [(triphos)Rh(C_6H_5)(C_2H_4)] (5). This yellow complex was prepared in ca. 85% yield as described for **4** except for substitution of LiPh (ca. 2 M in 75:25 C_6H_6–Et_2O, 1.25 mL, 2.5 mmol) for LiMe and for addition of *n*-heptane (100 mL) to complete the precipitation. Anal. Calcd for $C_{49}H_{48}P_3Rh$: C, 70.67; H, 5.81; Rh, 12.36. Found: C, 70.54; H, 5.77; Rh, 12.31.

Reaction of 1 with CO. Carbon monoxide was bubbled into a saturated solution of **1** (1 g, 1.26 mmol) in THF (30 mL) for 30 min. After CO was replaced with nitrogen, *n*-heptane (20 mL) was added portionwise to the resulting deep red solution and rusty red crystals of **[(triphos)RhCl(CO)]** precipitated on standing (80% yield), which were collected by filtration and washed with

(38) Pruett, R. L.; Smith, J. A. *J. Org. Chem.* **1969**, *34*, 327.
(39) Hewertson, W.; Watson, h. R. *J. Chem. Soc.* **1962**, 1490.
(40) Cramer, R. *Inorg. Synth.* **1974**, *15*, 14.
(41) Castellano, S.; Bothner-By, A. A. *J. Chem. Phys.* **1964**, *41*, 3863.
(42) Stephenson, D. S.; Binsch, G. *J. Magn. Reson.* **1980**, *37*, 395, 409.

n-pentane. Anal. Calcd for $C_{42}H_{39}ClOP_3Rh$: C, 63.77; H, 4.97; Rh, 13.01. Found: C, 63.66; H, 5.01; Rh, 12.95.

Reaction of 2 (or 3) with CO. Under a carbon monoxide atmosphere **2** (or **3**) (0.5 mmol) was dissolved in THF (20 mL) at −28 °C (2-propanol–ice bath). Within 2 h the starting product dissolved to give a yellow solution. Portionwise addition of *n*-heptane (90 mL) led to the precipitation of yellow crystals of **[(triphos)Rh(COEt)(CO)] (7)** (60% yield), which were collected by filtration and washed with *n*-pentane. Anal. Calcd for $C_{45}H_{44}O_2P_3Rh$: C, 66.51; H, 5.46; Rh, 12.66. Found: C, 66.46; H, 5.38; Rh, 12.58. IR: 1630 (ν(C=O)), 1890 cm^{-1} (ν(C≡O)).

Reaction of 4 (or 5) with CO. Under a carbon monoxide atmosphere **4** (or **5**) (0.5 mmol) was dissolved in THF (20 mL). After 2 h on addition of 1-butanol (10 mL) and *n*-heptane (50 mL) yellow crystals of **[(triphos)Rh(COCH$_3$)(CO)] (6)** or **[(triphos)Rh(COPh)(CO)] (8)** precipitated in ca. 75% yield, respectively. They were collected by filtration and washed with *n*-pentane. Anal. Calcd for $C_{44}H_{42}O_2P_3Rh$: C, 66.17; H, 5.30; Rh, 12.88. Found: C, 66.08; H, 5.23; Rh, 12.73. Calcd for $C_{49}H_{44}O_2P_3Rh$: C, 68.38; H, 5.15; Rh, 11.96. Found: C, 68.28; H, 5.11; Rh, 11.95. IR: **6**, 1600 (ν(C=O)), 1897 cm^{-1} (ν(C≡O)); **8**, 1600 (ν(C=O), 1905 cm^{-1} (ν(C≡O)).

Preparation of [(triphos)Rh(C$_2$H$_5$)(CO)] (9). EtMgBr (2 M in THF, 0.3 mL, 0.6 mmol) was syringed into a saturated solution of [(triphos)RhCl(CO)] (0.39 g, 0.5 mmol) in THF (30 mL). After 1 h the resulting orange solution was concentrated to 10 mL and the unreacted starting product eliminated by filtration. Addition of ethanol (20 mL) and *n*-heptane (20 mL) gave orange crystals in 30% yield, which were filtered off and washed with *n*-pentane. Anal. Calcd for $C_{44}H_{44}OP_3Rh$: C, 67.35; H, 5.65; Rh, 13.11. Found: C, 67.39; H, 5.66; Rh, 13.03. IR: 1888 cm^{-1} (ν(C=O)).

Preparation of [(triphos)Rh(CH$_3$)(CO)] (10). LiMe (1.6 M in THF, 1.5 mL, 2.4 mmol) was syringed into a suspension of [(triphos)RhCl(CO)] (0.39 g, 0.5 mmol) in THF (30 mL). Addition of ethanol (20 mL) and *n*-heptane (20 mL) to the resulting red-brown solution gave orange crystals in 40% yield, which were filtered off and washed with *n*-pentane. Anal. Calcd for $C_{43}H_{42}OP_3Rh$: C, 67.01; H, 5.49; Rh, 13.35. Found: C, 66.84; H, 5.36; Rh, 13.23. IR: 1895 cm^{-1} (ν(C≡O)).

Preparation of [(triphos)Rh(C$_6$H$_5$)(CO)] (11). This yellow complex was prepared in ca. 35% yield as described for **9** except for substitution of LiPh (ca. 2 M in 75:25 C_6H_6–Et_2O, 0.35 mL, 0.7 mmol) for EtMgBr. Anal. Calcd for $C_{48}H_{44}OP_3Rh$: C, 69.23; H, 5.33; Rh, 12.35. Found: C, 69.13; H, 5.28; Rh, 12.26. IR: 1915 cm^{-1} (ν(C≡O)).

Reaction of 9, 10, or 11 with CO. Under a carbon monoxide atmosphere 0.5 mmol of **9**, **10**, or **11** was dissolved in THF (20 mL). After 30 min addition of 1-butanol (10 mL) and *n*-heptane (50 mL) gave yellow crystals of **7**, **6**, or **8**, respectively, in ca. 80% yield.

Reaction of 1 with H$_2$. A THF (20 mL) solution of **1** (0.39 g, 0.5 mmol) was stirred in a 100-mL vessel under 1 atm of dihydrogen at room temperature for 1 h. The GC analysis of the gas phase revealed the presence of C_2H_6 and C_2H_4 in traces. Beige crystals of **[(triphos)Rh(H)$_2$Cl] (12)** precipitated on addition of ethanol (20 mL) and *n*-heptane (20 mL) to the solution; yield 55%. They were washed with a 1:1 mixture of *n*-pentane–ethanol and with *n*-pentane. Anal. Calcd for $C_{41}H_{41}ClP_3Rh$: C, 64.37; H, 5.40; Rh, 13.45. Found: C, 64.22; H, 5.38; Rh, 13.36. IR: 1960 cm^{-1} (ν(Rh—H)).

Reaction of 2, 3, 4, and 5 with H$_2$. The analogous treatment of all of the other ethylene complexes with hydrogen gave white crystals of **[(triphos)RhH$_3$] (13)** almost in quantitative yields. While the GC analysis of the gas phases revealed the presence of C_2H_6 for **2** and **3** and CH_4 for **4**, the analysis of the liquid phase of **5** showed C_6H_6.

Reaction of 6, 7, and 8 with H$_2$. When an analogous treatment was applied to the σ-acyl carbonyls **6**, **7**, and **8**, except for a temperature increase to 68 °C, yellow crystals of **[(triphos)RhH(CO)] (14)** were obtained almost in quantitative yields. The GC analysis of the resulting solutions revealed the presence of CH_3CHO, C_2H_5CHO, and C_6H_5CHO for **6**, **7**, and **8**, respectively.

Reaction of 9, 10, and 11 with H$_2$. Working up as above the σ-organyl carbonyls **9**, **10**, and **11** also gave **14** almost in quantitative yields. While the GC analysis of the gas phase revealed the presence of C_2H_6 for **9** CH_4 for **10**, the analysis of the solution of **11** showed C_6H_6.

Preparation of [(triphos)Rh(η^2-DMAD)]BPh$_4$ (15). A mixture of **1** (1 g, 1.26 mmol) and dimethyl acetylenedicarboxylate (DMAD) (0.28 mL, 2 mmol) in CH_2Cl_2 (20 mL) was allowed to react for 1 h. On addition of $NaBPh_4$ (0.51 g, 1.5 mmol) in ethanol (30 mL) and partial evaporation of the solvent red crystals precipitated in 95% yield. They were filtered off and washed with ethanol and petroleum ether. Anal. Calcd for $C_{71}H_{65}BO_4P_3Rh$: C, 71.72; H, 5.51; Rh, 8.65. Found: C, 71.68; H, 5.48; Rh, 8.58. IR: 1680 (ν(C=O)), 1750 cm^{-1} (ν(C≡C)). Λ_M = 45 cm^2 Ω^{-1} mol^{-1}.

Reaction of 15 with H$_2$. Hydrogen was bubbled into a THF (20 mL) solution of **15** (0.59 g, 0.5 mmol) for 1 h. Monitoring the reaction by GC showed the formation of dimethyl succinate. When the resulting orange solution was eluted with 1-butanol, yellow crystals of **[(triphos)RhH(μ-H)$_2$HRh(triphos)](BPh$_4$)$_2$ (16)** precipitated in 68% yield.

Reaction of 15 with CO. Carbon monoxide was bubbled into a THF (25 mL) solution of **15** (0.36 g, 0.3 mmol) for 45 min. On addition of 1-butanol (30 mL) and partial evaporation of the solvent under nitrogen yellow crystals of **[(triphos)Rh(CO)$_2$]BPh$_4$ (17)** precipitated in 90% yield. By treatment of **17** in THF with excess DMAD, **15** was recovered in almost quantitative yield.

Preparation of [(triphos)Rh(CO)(C$_2$H$_4$)]BPh$_4$ (18). A. A mixture of **17** (0.33 g, 0.3 mmol) and Me_3NO (0.09 g, 1.2 mmol) in THF (35 mL) was stirred under ethylene for 1 h. The excess of Me_3NO was eliminated by filtration and the resulting orange solution eluted with ethanol (30 mL). Orange powder was obtained on concentration to half volume. This was identified as a 3:2 mixture of **18** and **[{(OPPh$_2$CH$_2$)C(CH$_3$)(CH$_2$PPh$_2$)$_2$}Rh(CO)$_2$]BPh$_4$** (on the basis of NMR integration). $^{31}P\{^1H\}$ NMR (121.42 MHz, CD_3COCD_3, 20 °C): 32.18 ppm (2 P, doublet, J(PRh) = 194.5 Hz), 28.05 ppm (1 P, singlet, P=O). IR (Nujol mull): 2033 cm^{-1} (ν(C≡O)).

B. Neat $HOSO_2CF_3$ (0.03 mL, 0.33 mmol) was syringed into a stirred solution of **14** (0.23 g, 0.3 mmol) in THF (20 mL) under ethylene. After 2 h addition of ethanol (30 mL) gave yellow crystals in 77% yield. They were filtered off and washed with ethanol and petroleum ether. Anal. Calcd for $C_{68}H_{63}BOP_3Rh$: C, 74.05; H, 5.76; Rh, 9.33. Found: C, 73.81; H, 5.69; Rh, 9.11. IR (Nujol mull): 2055 cm^{-1} (ν(C≡O)). Λ_M = 41 cm^2 Ω^{-1} mol^{-1}.

Preparation of [(triphos)Rh(H)$_2$(CO)]BPh$_4$ (19). For a workup as in the above method B, except for the substitution of nitrogen for an ethylene atmosphere, **19** was obtained as colorless crystals in 83% yield. Anal. Calcd for $C_{66}H_{61}BOP_3Rh$: C, 73.61; H, 5.71; Rh, 9.55. Found: C, 73.45; H, 5.74; Rh, 9.42. IR: 1962 (ν(Rh—H)), 2066 cm^{-1} (ν(C≡O)). Λ_M = 42 cm^2 Ω^{-1} mol^{-1}.

Isomerization of DMMA to DMFU by [(triphos)RhH]. Dimethyl maleate (15 mmol) was refluxed for 3 h under nitrogen in benzene (30 mL) in the presence of **2** (0.5 mmol). The GC analysis of the resulting solution evidenced the complete isomerization to dimethyl fumarate. On addition of *n*-heptane (40 mL) a mixture of [(triphos)RhH(η^2-DMFU)] and free DMFU precipitated. The rhodium complex was recovered in pure form by washing the precipitate with diethyl ether.[2h]

Isomerization of *cis*-Stilbene to *trans*-Stilbene by [(triphos)Rh]$^+$. A mixture of *cis*-stilbene (15 mmol), **1** (0.5 mmol), and $NaBPh_4$ (0.5 mmol), the last compound employed as a halogen scavenger, was heated at reflux temperature for 3 h under nitrogen in THF (30 mL). The GC analysis of the final solution evidenced the complete isomerization to *trans*-stilbene.

Catalytic Runs. Hydrogenations. Air was evacuated from a 125-mL stainless steel autoclave containing the catalyst; then the substrate and the solvent were introduced by suction. Hydrogen was added up to the desired pressure, and the autoclave was then rocked and heated at the selected temperature. The conversion was determined from the crude product by GC analysis with appropriate columns (Al203 PLOT capillary column, 50 m, i.d. 0.32 mm, for 1-hexene hydrogenation; packed column (2 m) containing free fatty acid phase (5%) on Chromosorb G AW-DMCS for the other substrates).

Hydroformylations. The procedure was analogous to that reported for hydrogenation. The product composition was evaluated by GC analysis with the appropriate amount of 1-hexanol as the internal standard (packed column, 2 m, containing Ucon oil LB 550-X (15%) on Chromosorb W). The hydrocarbon

Table XI. Summary of Crystal Data for 1

formula	$C_{43}H_{43}ClP_3Rh$
mol wt	791.10
cryst size	0.41 × 0.15 × 0.03
cryst syst	orthorhombic
space group	$Pb2_1a$ (No. 29)
a, Å	20.452 (4)
b, Å	17.348 (2)
c, Å	10.651 (5)
α, β, γ, deg	90.00
V, Å^3	3779.0
Z	4
d(calcd), g cm^{-3}	1.39
μ(Mo Kα), cm^{-1}	6.31
diffractometer	Philips PW1100
radiation	graphite-monochromated Mo Kα, λ = 0.71069 Å
scan type	ω–2θ
2θ range, deg	5–50
scan width	0.8
scan speed, deg s^{-1}	0.04
total no. of data	3753
no. of unique data, $I \geq 3\sigma(I)$	1186
no. of params	148
R	0.056
R_w	0.057
transmissn factors: max, min	0.984–0.919

composition was evaluated as reported in the hydrogenation procedure. The hydroformylation, hydrogenation, and isomerization products were identified by comparison with authentic samples or by GC–MS spectra on an OV-101 column (25 m).

X-ray Data Collection and Structure Determination of 1. Crystals suitable for an X-ray diffraction analysis were obtained by slow diffusion of ethanol vapors into a CH_2Cl_2 solution of 1 maintained under an ethylene atmosphere at room temperature. A summary of crystal and intensity data is reported in Table XI. All X-ray measurements were performed on a Philips PW1100 automated four-circle diffractometer using Mo Kα radiation monochromatized with a graphite crystal. The cell parameters were determined by least-squares refinement of the setting angles of 25 carefully centered reflections. As a general procedure, three standard reflections were collected every 2 h (no decay of intensities was observed in any case). Intensity data were corrected for Lorentz-polarization effects. Atomic scattering factors were those reported by Cromer and Waber[43] with anomalous dispersion corrections taken from ref 44. All the calculations were done on a Sel 32/77 computer, installed in our institute, by using the SHELX 76 program.[45] The structure was solved by Patterson and Fourier techniques. Refinement was done by full-matrix least-squares calculations initially with isotropic thermal parameters. Anisotropic thermal parameters were used only for the Rh, P, and Cl atoms. An absorption correction by the numerical-integration method was applied (faces 100, 010, 001).[45] The phenyl rings were treated as rigid bodies of D_{6h} symmetry with C–C distances fixed at 1.395 Å and calculated hydrogen atom positions (C–H = 0.96 Å). None of the residual peaks detected in the Fourier difference map allowed us to localize the ethylene hydrogen atoms.

(43) Cromer, D. T.; Waber, J. T. *Acta Crystallogr.* **1965**, *18*, 104.
(44) *International Tables of Crystallography*; Kynoch: Birmingham, England, 1974; Vol. 4.
(45) Sheldrick, G. M. "SHELX76 Program for Crystal Structure Determinations"; University of Cambridge: Cambridge, England, 1976.

Table XII. Final Positional Parameters (×10^4) for 1

atom	x	y	z
Rh	1475 (1)	1850 (1)	2513 (2)
Cl	1801 (3)	533 (4)	1925 (7)
P1	1067 (3)	2980 (4)	3106 (7)
P2	2059 (3)	1783 (6)	4412 (5)
P3	2376 (3)	2509 (4)	1613 (6)
C1	1716 (10)	3712 (14)	3386 (22)
C2	2229 (11)	2765 (13)	4941 (21)
C3	2779 (10)	3083 (13)	2886 (19)
C4	2348 (13)	3388 (15)	3963 (23)
C5	2743 (11)	4029 (14)	4551 (21)
C6	484 (11)	1364 (13)	2466 (28)
C7	670 (11)	1644 (13)	1195 (21)
C1,1	490 (9)	3465 (9)	2028 (14)
C2,1	−163 (9)	3235 (9)	2097 (14)
C3,1	−616 (9)	3519 (9)	1236 (14)
C4,1	−417 (9)	4034 (9)	305 (14)
C5,1	236 (9)	4264 (9)	235 (14)
C6,1	689 (9)	3979 (9)	1097 (14)
C1,2	577 (8)	3050 (8)	4578 (16)
C2,2	396 (8)	2401 (8)	5268 (16)
C3,2	51 (8)	2486 (8)	6390 (16)
C4,2	−113 (8)	3220 (8)	6821 (16)
C5,2	68 (8)	3869 (8)	6131 (16)
C6,2	413 (8)	3784 (8)	5009 (16)
C1,3	1663 (7)	1295 (9)	5736 (11)
C2,3	1320 (7)	625 (9)	5439 (11)
C3,3	975 (7)	233 (9)	6371 (11)
C4,3	973 (7)	511 (9)	7600 (11)
C5,3	1316 (7)	1181 (9)	7897 (11)
C6,3	1661 (7)	1573 (9)	6965 (11)
C1,4	2895 (8)	1348 (10)	4569 (13)
C2,4	3238 (8)	1394 (10)	5698 (13)
C3,4	3877 (8)	1116 (10)	5771 (13)
C4,4	4173 (8)	794 (10)	4715 (13)
C5,4	3830 (8)	749 (10)	3585 (13)
C6,4	3191 (8)	1026 (10)	3512 (13)
C1,5	2233 (8)	3196 (11)	345 (15)
C2,5	2620 (8)	3845 (11)	133 (15)
C3,5	2511 (8)	4305 (11)	−921 (15)
C4,5	2014 (8)	4116 (11)	−1763 (15)
C5,5	1626 (8)	3467 (11)	−1551 (15)
C6,5	1736 (8)	3007 (11)	−498 (15)
C1,6	3052 (7)	2008 (9)	848 (14)
C2,6	3709 (7)	2161 (9)	1094 (14)
C3,6	4196 (7)	1769 (9)	437 (14)
C4,6	4026 (7)	1223 (9)	−468 (14)
C5,6	3369 (7)	1069 (9)	−714 (14)
C6,6	2882 (7)	1462 (9)	−56 (14)

Atomic coordinates for all the non-hydrogen atoms are given in Table XII.

Acknowledgment. We are grateful to Prof. A. Vacca for helpful discussions and to Dr. C. Mealli for an X-ray crystal structure determination. We wish to thank also the Conselleria de Culture of Generalitat Valenciana for a grant that made J.A.R.'s stay in Firenze possible.

Supplementary Material Available: Refined anisotropic and isotropic temperature factors (Table XIII) and final positional parameters for hydrogen atoms for 1 (Table XIV) (3 pages); a listing of observed and calculated structure factors for 1 (7 pages). Ordering information is given on any current masthead page.